



1 Hydrothermal activity lowers trophic diversity in Antarctic sedimented hydrothermal vents

2

3 James B. Bell^{1,2}, William D. K. Reid³, David A. Pearce⁴, Adrian G. Glover², Christopher J. Sweeting⁵,

4 Jason Newton⁶, & Clare Woulds^{1*}

5

6 ¹School of Geography & Water@Leeds, University of Leeds, LS2 9JT, UK.

7 ²Life Sciences Dept., Natural History Museum, Cromwell Rd, London SW7 5BD, UK

8 ³Ridley Building, School of Biology, Newcastle University, NE1 7RU, UK

9 ⁴Applied Sciences, Northumbria University, Newcastle, NE1 8ST, UK

10 ⁵Ridley Building, School of Marine Science and Technology, Newcastle University, NE1 7RU, UK

11 ⁶NERC Life Sciences Mass Spectrometry Facility, SUERC, East Kilbride G75 0QF, UK

12

13 * E-mail: c.woulds@leeds.ac.uk

14

15 Keywords: Stable Isotopes; Trophic Niche; Sedimented; Hydrothermal; Southern Ocean;

16 Microbial; 16S; PLFA



17 Abstract

18

19 Sedimented hydrothermal vents are those in which hydrothermal fluid is discharged through
20 sediments and are among the least studied deep-sea ecosystems. We present a combination of
21 microbial and biochemical data to assess trophodynamics between and within hydrothermally
22 active and off-vent areas of the Bransfield Strait (1050 – 1647m depth). Microbial composition,
23 biomass and fatty acid signatures varied widely between and within vent and non-vent sites and
24 provided evidence of diverse metabolic activity. Several species showed diverse feeding
25 strategies and occupied different trophic positions in vent and non-vent areas. Stable isotope
26 values of consumers were generally not consistent with feeding structure morphology. Niche
27 area and the diversity of microbial fatty acids reflected trends in species diversity and was
28 lowest at the most hydrothermally active site. Faunal utilisation of chemosynthetic activity was
29 relatively limited but was detected at both vent and non-vent sites as evidenced by carbon and
30 sulphur isotopic signatures, suggesting that hydrothermal activity can affect trophodynamics
31 over a much wider area than previously thought.

32



33 Section 1. Introduction

34

35 Sedimented hydrothermal vents (SHVs, a.k.a. Sediment-hosted hydrothermal vents), the
36 product of subsurface mixing between hydrothermal fluid and ambient seawater within the
37 sediment, are physically more similar to non-hydrothermal deep-sea habitats than they are to
38 high temperature, hard substratum vents (Bemis et al. 2012, Bernardino et al. 2012). This means
39 that, whilst they can host chemosynthetic obligate species, they can also be colonised by non-
40 specialist fauna, potentially offering an important metabolic resource in the nutrient-limited
41 deep-sea (Levin et al. 2009, Dowell et al. 2016). Sedimented vents have also been suggested to
42 act as evolutionary bridges between hard substratum vents and methane seeps (Kiel 2016). To
43 utilise in situ production at SHVs, fauna must overcome the environmental stress associated
44 with high-temperature, acidic and toxic conditions (Levin et al. 2013, Gollner et al. 2015). The
45 combination of elevated toxicity and in-situ organic matter (OM) production results in a
46 different complement of ecological niches between vents and background conditions that elicits
47 compositional changes along a productivity-toxicity gradient (Bernardino et al. 2012, Gollner et
48 al. 2015, Bell et al. 2016b). Hydrothermal sediments offer different relative abundances of
49 chemosynthetic and photosynthetic organic matter, depending upon supply of surface-derived
50 primary productivity, which may vary with depth and latitude, and levels of hydrothermal
51 activity (Tarasov et al. 2005). In shallow environments (<200 m depth), where production of
52 chemosynthetic and photosynthetic organic matter sources can co-occur, consumption may still
53 favour photosynthetic OM over chemosynthetic OM as this does not require adaptations to
54 environmental toxicity (Kharlamenko et al. 1995, Tarasov et al. 2005, Sellanes et al. 2011). The
55 limited data available concerning trophodynamics at deep-sea SHVs, from the Arctic, indicate
56 that diet composition varies widely between taxa, ranging between 0 – 87 % contribution from



57 chemosynthetic OM (Sweetman et al. 2013). Thus, understanding of the significance of
58 chemosynthetic activity in these settings is very limited.

59

60 Sedimented hydrothermal vents host diverse microbial communities (Teske et al. 2002,
61 Kallmeyer & Boetius 2004). Microbial communities are a vital intermediate between
62 hydrothermal fluid and metazoan consumers, and thus their composition and isotopic
63 signatures are of direct relevance to metazoan food webs. The heat flux associated with
64 hydrothermal activity provides thermodynamic benefits and constraints to microbial
65 communities (Kallmeyer & Boetius 2004, Teske et al. 2014) whilst accelerating the degradation
66 of organic matter, giving rise to a wide variety of compounds including hydrocarbons and
67 organic acids (Martens 1990, Whiticar & Suess 1990, Dowell et al. 2016). Microbial aggregations
68 are commonly visible on the sediment surface at SHVs (Levin et al. 2009, Sweetman et al. 2013,
69 Dowell et al. 2016). However, active communities are also distributed throughout the underlying
70 sediment layers, occupying a wide range of geochemical and thermal niches (reviewed by Teske
71 et al. 2014). This zonation in microbial function and composition is very strong and has been
72 extensively studied in Guaymas basin hydrothermal sediments. Sedimented chemosynthetic
73 ecosystems may present several sources of organic matter to consumers (Bernardino et al. 2012,
74 Sweetman et al. 2013, Yamanaka et al. 2015) and the diverse microbial assemblages can support
75 a variety of reaction pathways, including methane oxidation, sulphide oxidation, sulphate
76 reduction and nitrogen fixation (Teske et al. 2002, Dekas et al. 2009, Jaeschke et al. 2014).
77 Phospholipid fatty acid (PLFA) analysis can be used to describe recent microbial activity and
78 $\delta^{13}\text{C}$ signatures (Boschker & Middelburg 2002, Yamanaka & Sakata 2004, Colaço et al. 2007).
79 Although it can be difficult to ascribe a PLFA to a specific microbial group or process, high
80 relative abundances of certain PLFAs can be strongly indicative of chemoautotrophy (Yamanaka



81 & Sakata 2004, Colaço et al. 2007), and can support an understanding of microbial ecosystem
82 function in hydrothermal sediments (e.g. in western pacific vents, see Yamanaka & Sakata 2004).
83
84 Macrofaunal assemblages of the Bransfield SHVs were strongly influenced by hydrothermal
85 activity (Bell et al. 2016b). Bacterial mats were widespread across Hook Ridge, where variable
86 levels of hydrothermal activity were detected (Aquilina et al. 2013). Populations of siboglinid
87 polychaetes (*Sclerolinum contortum* and *Siboglinum* sp.), were found at Hook Ridge and non-
88 hydrothermally active sites (Sahling et al. 2005, Georgieva et al. 2015, Bell et al. 2016b). These
89 species are known to harbour chemoautotrophic endosymbionts (Schmaljohann et al. 1990,
90 Eichinger et al. 2013, Rodrigues et al. 2013). Stable isotope analysis (SIA) is a powerful tool to
91 assess spatial and temporal patterns in faunal feeding behaviour and has been used to study
92 trophodynamics and resource partitioning in other SHVs, predominately in the Pacific (Fry et al.
93 1991, Levin et al. 2009, Portail et al. 2016). Stable isotopic analyses provide inferential measures
94 of different synthesis pathways and can elucidate a wide range of autotrophic or feeding
95 behaviours. Carbon and sulphur isotopes are used here to delineate food sources and nitrogen
96 is used as a measure of trophic position. The signature of source isotope ratios ($\delta^{13}\text{C}$ & $\delta^{34}\text{S}$) is
97 influenced by the isotopic ratio of the chemical substrate, and the fractionation associated with
98 the metabolic process involved and thus, different fixation pathways elicit different isotopic
99 signatures, even when they utilise the same source (e.g. DIC) (Fry et al. 1991). Possible $\delta^{13}\text{C}$
100 isotopic values of sources in the Bransfield Strait include: \sim -40 ‰ for thermogenic methane; \sim -
101 27 ‰ for suspended particulate matter or \sim -15 ‰ for ice algae (Whiticar & Suess 1990, Mincks
102 et al. 2008, Henley et al. 2012, Young et al. 2013). As an example, *Siboglinum* spp. can use a range
103 of resources, including methane or dissolved organic matter (Southward et al. 1979,
104 Schmaljohann et al. 1990, Thornhill et al. 2008, Rodrigues et al. 2013), making SIA an ideal way
105 in which to examine resource utilisation in these settings (Levin et al. 2009, Soto 2009). We also



106 apply the concept of an isotopic niche (Layman et al. 2007) whereby species or community
107 trophic activity is inferred from the distribution of stable isotopic data in two or three
108 dimensional isotope space.

109

110 Hypotheses

111

112 We used a combination of microbial diversity data based sequencing and compound specific
113 isotopic analyses and bulk isotopic data from sediment, microbial, macro- and megafaunal
114 samples to investigate resource utilisation, niche partitioning and trophic structure at vent and
115 background sites in the Bransfield Strait to test the following hypotheses: 1) Siboglinid species
116 subsist upon chemosynthetically-derived OM; 2) Chemosynthetic organic matter will be a
117 significant food source at SHVs; 3) Stable isotope signatures will reflect a-priori functional
118 designations defined by faunal morphology and 4) Fauna will have distinct niches between vents
119 and background areas.



120 Section 2. Materials and Methods

121

122 2.1. Sites and Sampling

123

124 Samples were collected; during RRS *James Cook* cruise JC55 in the austral summer of 2011 (Tyler
125 et al. 2011), from three raised edifices along the basin axis (Hook Ridge, the Three Sisters and
126 The Axe) and one off-axis site in the Bransfield Strait (1024 – 1311m depth; Fig. 1; Table 1). We
127 visited two sites of variable hydrothermal activity (Hook Ridge 1 and 2) and three sites where
128 hydrothermal activity was not detected (Three Sisters, the Axe and an Off-Axis site) (Aquilina et
129 al. 2013). Of the two hydrothermal sites, Hook Ridge 2 was had higher hydrothermal fluid
130 advection rates and pore fluid temperature but lower concentrations of sulphide and methane
131 (Dähmann et al. 2001, Aquilina et al. 2013, Aquilina et al. 2014).

132

133 Samples were collected with a series of megacore deployments, using a Bowers & Connelly
134 dampened megacorer (1024 – 1311 m depth) and a single Agassiz trawl at Hook Ridge (1647 m
135 depth). With the exception of salps, all microbial and faunal samples presented here were from
136 megacore deployments. For a detailed description of the megacore sampling programme and
137 macrofaunal communities, see Bell et al. (2016b). Sampling consisted of 1 – 6 megacore
138 deployments per site, with 2 – 5 tubes pooled per deployment (Bell et al. 2016b). Cores were
139 sliced into 0 – 5 cm and 5 – 10 cm partitions and macrofauna were retained on a 300µm sieve.
140 Residues were preserved in either 80 % ethanol or 10 % buffered formalin initially and then
141 stored in 80% ethanol after sorting (Bell et al. 2016b). Fauna were sorted to species/
142 morphospecies level (for annelid and bivalve taxa); family level (for peracarids) and higher
143 levels for less abundant phyla (e.g. echiurans). Salps were collected using an Agassiz trawl and
144 samples were immediately picked and frozen at -80 °C and subsequently freeze-dried.



145

146 2.2. Microbiology Sequencing

147

148 Samples of surface sediment (0 – 1 cm below seafloor (cmbsf)) were taken from megacores the
149 two Hook Ridge sites and the off-axis site and frozen (-80°C). DNA was extracted from the
150 sediment by Mr DNA (Shallowater, TX, USA) using an in-house standard 454 pipeline. The
151 resultant sequences were trimmed and sorted using default methods in Geneious (v.9.1.5 with
152 RDP v.2.8 and Krona v.2.0) and analysed in the Geneious '16 Biodiversity Tool'
153 (<https://16s.geneious.com/16s/help.html>); (Wang et al. 2007, Ondov et al. 2011, Biomatters
154 2014).

155

156 2.3. Phospholipid Fatty Acids

157

158 Samples of 3 – 3.5 g of freeze-dried sediment from Hook Ridge 1 & 2, the off-vent site and the
159 Three Sisters were analysed at the James Hutton Institute (Aberdeen, UK) following the
160 procedure detailed in Main et al. (2015), which we summarise below. Samples were from the
161 top 1 cm of sediment for all sites except Hook Ridge 2 where sediment was pooled from two core
162 slices (0 – 2 cm), due to sample mass limitations. Lipids were extracted following a method
163 adapted from Bligh (1959), using a single phase mixture of chloroform: methanol: citrate buffer
164 (1:2:0.8 v-v:v). Lipids were fractionated using 6 ml ISOLUTE SI SPE columns, preconditioned
165 with 5 ml chloroform. Freeze-dried material was taken up in 400 µL of chloroform; vortex mixed
166 twice and allowed to pass through the column. Columns were washed in chloroform and acetone
167 (eluates discarded) and finally 10 ml of methanol. Eluates were collected, allowed to evaporate
168 under a N₂ atmosphere and frozen (-20 °C).

169



170 PLFAs were derivitised with methanol and KOH to produce fatty acid methyl esters (FAMES).
171 Samples were taken up in 1 mL of 1:1 (v:v) mixture of methanol and toluene. 1 mL of 0.2 M KOH
172 (in methanol) was added with a known quantity of the C19 internal standard (nonadecanoic
173 acid), vortex mixed and incubated at 37 °C for 15 min. After cooling to room temperature, 2 mL
174 of isohexane:chloroform (4:1 v:v), 0.3 mL of 1 M acetic acid and 2 mL of deionized water was
175 added to each vial. The solution was mixed and centrifuged and the organic phase transferred to
176 a new vial and the remaining aqueous phase was mixed and centrifuged again to further extract
177 the organic phase, which was combined with the previous. The organic phases were evaporated
178 under a N₂ atmosphere and frozen at -20 °C.

179

180 Samples were taken up in isohexane to perform gas chromatography-combustion-isotope ratio
181 mass spectrometry (GC-C-IRMS). The quantity and $\delta^{13}\text{C}$ values of individual FAMES were
182 determined using a GC Trace Ultra with combustion column attached via a GC Combustion III to
183 a Delta V Advantage isotope ratio mass spectrometer (Thermo Finnigan, Bremen). The $\delta^{13}\text{C}_{\text{VPDB}}$
184 values (‰) of each FAME were calculated with respect to a reference gas of CO₂, traceable to
185 IAEA reference material NBS 19 TS-Limestone. Measurement of the Indiana University reference
186 material hexadecanoic acid methyl ester (certified $\delta^{13}\text{C}_{\text{VPDB}} -30.74 \pm 0.01\text{‰}$) gave a value of
187 $30.91 \pm 0.31\text{‰}$ (mean \pm s. d., n = 51). Combined areas of all mass peaks (m/z 44, 45 and 46),
188 following background correction, were collected for each FAME. These areas, relative to the
189 internal C19:0 standard, were used to quantify the 34 most abundant FAMES and related to the
190 PLFAs from which they are derived (Thornton et al. 2011).

191

192 Bacterial biomass was calculated using transfer functions from the total mass of four PLFAs
193 (i14:0, i15:0, a15:0 and i16:0), estimated at 14 % of total bacterial PLFA, which in turn is
194 estimated at 5.6 % of total bacterial biomass (Boschker & Middelburg 2002).



195

196 2.4. Bulk Stable Isotopes

197

198 All bulk isotopic analyses were completed at the East Kilbride Node of the Natural Environment
199 Research Council Life Sciences Mass Spectrometry Facility. Specimens with carbonate structures
200 (e.g. bivalves) were physically decarbonated and all specimens were rinsed in de-ionised water
201 (e.g. to remove soluble precipitates such as sulphates) and cleaned of attached sediment before
202 drying. Specimens dried for at least 24 hours at 50°C and weighed (mg, correct to 3 d.p.) into tin
203 capsules and stored in a desiccator whilst awaiting SIA. Samples were analysed by continuous
204 flow isotope ratio mass spectrometer using a Vario-Pyro Cube elemental analyser (Elementar),
205 coupled with a Delta Plus XP isotope ratio mass spectrometer (Thermo Electron). Each of the
206 runs of CN and CNS isotope analyses used laboratory standards (Gelatine and two amino acid-
207 gelatine mixtures) as well as the international standard USGS40 (glutamic acid). CNS
208 measurements used the internal standards (MSAG2: (Methanesulfonamide/ Gelatine and M1:
209 Methionine) and the international silver sulphide standards IAEA-S1, S2 and S3. All sample runs
210 included samples of freeze-dried, powdered *Antimora rostrata* (ANR), an external reference
211 material used in other studies of chemosynthetic ecosystems (Reid et al. 2013, Bell et al. 2016a),
212 used to monitor variation between runs and instruments (supplementary file 1). Instrument
213 precision (S.D.) for each isotope measured from ANR was 0.42 ‰, 0.33 ‰ and 0.54 ‰ for
214 carbon, nitrogen and sulphur respectively. The reference samples were generally consistent
215 except in one of the CNS runs, which showed unusual $\delta^{15}\text{N}$ measurements (S1), so faunal $\delta^{15}\text{N}$
216 measurements from this run were excluded as a precaution. Stable isotope ratios are all reported
217 in delta (δ) per mil (‰) notation, relative to international standards: V-PDB ($\delta^{13}\text{C}$); Air ($\delta^{15}\text{N}$)
218 and V-CDT ($\delta^{34}\text{S}$). Machine error, relative to these standards ranged 0.01 – 0.23 for $\delta^{13}\text{C}$, for 0.01
219 – 0.13 $\delta^{15}\text{N}$ and 0.13 – 3.04 for $\delta^{34}\text{S}$. One of the Sulphur standards (Ag₂S IAEA: S2) had a notable



220 difference from the agreed measurements, suggesting either a compromised standard or poor
221 instrument precision. This error was not observed in other standards, or the reference material
222 used, but given the uncertainty here; only $\delta^{34}\text{S}$ differences greater than 3 ‰ are considered as
223 being significant.

224

225 A combination of dual- ($\delta^{13}\text{C}$ & $\delta^{15}\text{N}$, 319 samples) and tri-isotope ($\delta^{13}\text{C}$, $\delta^{15}\text{N}$ & $\delta^{34}\text{S}$, 83 samples)
226 techniques was used to describe bulk isotopic signatures of 43 species of macrofauna (35 from
227 non-vent sites, 19 from vent sites and 11 from both), 3 megafaunal taxa and sources of organic
228 matter. Samples submitted for carbon and nitrogen (CN) analyses were pooled if necessary to
229 achieve an optimal mass of 0.7 mg (\pm 0.5 mg). Where possible, individual specimens were kept
230 separate in order to preserve variance structure within populations but in some cases, low
231 sample mass meant individuals had to be pooled (from individuals found in replicate
232 deployments). Optimal mass for Carbon-Nitrogen-Sulphur (CNS) measurements was 2.5 mg
233 (\pm 0.5 mg) and, as with CN analyses, specimens were submitted as individual samples or pooled
234 where necessary. Samples of freeze-dried sediment from each site were also submitted for CNS
235 analyses (untreated for NS and acidified with 6M HCl for C). Acidification was carried out by
236 repeated washing with acid and de-ionised water.

237

238 Specimens were not acidified. A pilot study, and subsequent results presented here, confirmed
239 that the range in $\delta^{13}\text{C}$ measurements between acidified (0.1M and 1.0M HCl) was within the
240 untreated population range, in both polychaetes and peracarids and that acidification did not
241 notably or consistently reduce $\delta^{13}\text{C}$ standard deviation (Table 2). In the absence of a large or
242 consistent treatment effect, the low sample mass, (particularly for CNS samples) was dedicated
243 to increasing replication and preserving integrity of $\delta^{15}\text{N}$ & $\delta^{34}\text{S}$ measurements instead of
244 separating carbon and nitrogen/ sulphur samples (Connolly & Schlacher 2013).



245

246 Formalin and ethanol preservation effects can both influence the isotopic signature of a sample
247 (Fanelli et al. 2010, Rennie et al. 2012). Taxa that had several samples of each preservation
248 method from a single site (to minimise intra-specific differences) were examined to determine
249 the extent of isotopic shifts associated with preservation effects. Carbon and nitrogen isotopic
250 differences between ethanol and formalin preserved samples ranged between 0.1 ‰ – 1.4 ‰
251 and 0.4 ‰ – 2.0 ‰ respectively. Differences across all samples were not significant (Paired t-
252 test, $\delta^{13}\text{C}$: $t = 2.10$, $df = 3$, $p = 0.126$ and $\delta^{15}\text{N}$: $t = 1.14$, $df = 3$, $p = 0.337$). Given the unpredictable
253 response of isotopic signatures to preservation effects (which also cannot be extricated from
254 within-site, intraspecific variation) it was not possible to correct isotopic data (Bell et al. 2016a).
255 This contributed an unavoidable, but generally quite small, source of error in these
256 measurements.

257

258 2.5. Statistical Analyses

259

260 All analyses were completed in the R statistical environment (R Core Team 2013). Carbon and
261 nitrogen stable isotopic measurements were divided into those from vent or non-vent sites and
262 averaged by taxa and used to construct a Euclidean distance matrix (Valls et al. 2014). This
263 matrix was used to conduct a similarity profile routine (SIMPROF, 10 000 permutations, $p = 0.05$,
264 Ward linkage) using the clustsig package (v1.0) (Clarke et al. 2008, Whitaker & Christmann
265 2013) to test for significant structure within the matrix. The resulting cluster assignments were
266 compared to a-priori feeding groups (Bell et al. 2016b) using a Spearman Correlation Test (with
267 9 999 Monte Carlo resamplings) using the coin package (v1.0-24) (Hothorn et al. 2015). Isotopic
268 signatures of species sampled from both vent and non-vent sites were also compared with a one-
269 way ANOVA with Tukey's HSD pairwise comparisons (following a Shapiro-Wilk normality test).



270

271 Mean faunal measurements of $\delta^{13}\text{C}$ & $\delta^{15}\text{N}$ were used to calculate Layman metrics for each site
272 (Layman et al. 2007), sample-size corrected standard elliptical area (SEAc) and Bayesian
273 posterior draws (SEA.B, mean of 10^5 draws \pm 95 % credibility interval) in the SIAR package
274 (v4.2) (Parnell et al. 2010, Jackson et al. 2011). Differences in SEA.B between sites were
275 compared in mixSIAR. The value of p given is the proportion of ellipses from group A that were
276 smaller in area than those from group B (e.g. if $p = 0.02$, then 2 % of posterior draws from group
277 A were smaller than the group B mean) and is considered to be a semi-quantitative measure of
278 difference in means (Jackson et al. 2011).



279 Section 3. Results

280

281 3.1. Differences in microbial composition along a hydrothermal gradient

282

283 A total of 28,767, 35,490 and 47,870 sequences were obtained from the off-axis site and the vent
284 sites, Hook Ridge 1 and 2, respectively. Bacteria comprised almost the entirety of each sample,
285 with Archaea being detected only in the Hook Ridge 2 sample (< 0.1 % of sequences). Hook Ridge
286 1 was qualitatively more similar to the off-axis site than Hook Ridge 2. Both Hook Ridge 1 (vent)
287 and the off-vent site, BOV (non-vent), were dominated by Proteobacteria (48 % and 61 % of
288 reads respectively; Fig. 2), whereas Flavobacteriia dominated Hook Ridge 2 (43 %, 7 – 12 %
289 elsewhere) with Proteobacteria accounting for a smaller percentage of sequences (36 %; Fig. 2).
290 By sequence abundance, Flavobacteriia were the most clearly disparate group between Hook
291 Ridge 2 and the other sites. Flavobacteriia were comprised of 73 genera at Hook Ridge 2, 60
292 genera at BOV and 63 genera at HR1, of which 54 genera were shared between all sites. Hook
293 Ridge 2 had 15 unique flavobacteriial genera but these collectively accounted for just 0.9% of
294 reads, indicating that compositional differences were mainly driven by relative abundance,
295 rather than taxonomic richness.

296

297 The most abundant genus from each site was *Arenicella* at BOV and HR1 (7.1 and 5.2 % of reads
298 respectively) and *Aestuariicola* at HR2 (6.9 % of reads). The four most abundant genera at both
299 BOV and HR1 were *Arenicella* (γ -proteobacteria), *Methylohalomonas* (γ -proteobacteria),
300 *Pasteuria* (Bacilli) & *Blastopirellula* (Planctomycetacia), though not in the same order, and
301 accounted for 17.2% and 16.0 % of reads respectively. The four most abundant genera at HR2,
302 accounting for 20.2 % of reads were *Aestuariicola*, *Lutimonas*, *Maritimimonas* & *Winogradskyella*



303 (all Flavobacteriia). The genera *Arenicella* and *Pasteuria* were the most relatively abundant
304 across all sites (2.2 % – 7.1 % and 1.7 % – 5.0 % of reads respectively).

305

306 3.2. Microbial fatty acids

307

308 A total of 37 sedimentary PLFAs were identified across all sites, in individual abundances
309 ranging between 0 % – 26.4 % of total PLFA (Table 3; Supplementary Fig 1). All lipid samples
310 were dominated by saturated and mono-unsaturated fatty acids (SFAs and MUFAs), comprising
311 91 % – 94 % of PLFA abundance per site. The most abundant PLFAs at each site were
312 16:0 (15.7 % – 26.4 %), 16:1 ω 7c (11.5 % – 20.0 %) and 18:1 ω 7 (4.8 % – 16.9 %; Table 3). PLFA
313 profiles from each of the non-vent sites sampled (Off-axis and the Three Sisters, 33 and 34 PLFAs
314 respectively) were quite similar (Table 3) and shared all but one compound (16:1 ω 11c, present
315 only at the non-vent Three Sisters site). Fewer PLFAs were enumerated from Hook Ridge 1 and
316 2 (31 and 23 respectively), including 3 PLFAs not observed at the non-vent sites (br17:0, 10-Me-
317 17:0 & 10-Me-18:0), which accounted for 0.5 % – 1.2 % of the total at these sites. Poly-
318 unsaturated algal biomarkers (20:5 ω 3 and 22:6 ω 3) were only detected at the non-vent site
319 (0.83 – 1.57 % of total FA abundance). Hook Ridge 2 had the lowest number of PLFAs and the
320 lowest total PLFA biomass of any site, though this was due in part to the fact that this sample
321 had to be pooled from the top 2 cm of sediment (top 1cm at other sites). Bacterial biomass was
322 highest at Hook Ridge 1 and ranged 85 mg C m⁻² – 535 mg C m⁻² (Table 3).

323

324 PLFA carbon isotopic signatures ranged -56 ‰ to -20 ‰ at non-vent sites and -42 ‰ to -8 ‰
325 at vent sites (Table 3). Weighted average $\delta^{13}\text{C}$ values were quite similar between the non-vent
326 sites and Hook Ridge 1 (-30.5 ‰ and -30.1 ‰ respectively), but were heavier at Hook Ridge 2
327 (-26.9 ‰; Table 3). Several of the PLFAs identified had a large range in $\delta^{13}\text{C}$ between samples



328 (including 16:1 ω 11t $\delta^{13}\text{C}$ range = 17.2 ‰ or 19:1 ω 8 $\delta^{13}\text{C}$ range = 19.1 ‰), even between the
329 non-vent sites (e.g. 18:2 ω 6, 9, $\Delta\delta^{13}\text{C}$ = 24.4; Table 3). Of the 37 PLFAs, 7 had a $\delta^{13}\text{C}$ range of >
330 10 ‰ but these were comparatively minor and individually accounted for 0 % – 4.9 % of total
331 abundance. Average $\delta^{13}\text{C}$ range was 6.3 ‰ and a further 11 PLFAs had a $\delta^{13}\text{C}$ range of > 5 ‰,
332 including some of the more abundant PLFAs, accounting for 36.8 ‰ – 46.6 % at each site. PLFAs
333 with small $\delta^{13}\text{C}$ ranges (< 5 ‰) accounted for 44.6 % – 54.4 % of total abundance at each site.

334

335 3.3. Description of bulk isotopic signatures

336

337 Most faunal isotopic signatures were within a comparatively narrow range ($\delta^{13}\text{C}$: -30 ‰ to -
338 20 ‰, $\delta^{15}\text{N}$: 5 ‰ to 15 ‰ and $\delta^{34}\text{S}$: 10 ‰ to 20 ‰) and more depleted isotopic signatures
339 were usually attributable to siboglinid species (Fig. 3). *Siboglinum* sp. (found at all non-vent
340 sites) had mean $\delta^{13}\text{C}$ and $\delta^{15}\text{N}$ values of -41.4 ‰ and -8.9 ‰ respectively and *Sclerolinum*
341 *contortum* (predominately from Hook Ridge 1 but found at both vent sites) had values of -
342 20.5 ‰ and -5.3‰ respectively. Some non-endosymbiont bearing taxa (e.g. macrofaunal
343 neotanaids from the off-axis site and megafaunal ophiuroids at Hook Ridge 2) also had notably
344 depleted $\delta^{15}\text{N}$ signatures (means -3.6‰ to 2.6 ‰ respectively; Fig. 3).

345

346 Isotopic signatures of sediment organic matter were similar between vents and non-vents for
347 $\delta^{13}\text{C}$ and $\delta^{15}\text{N}$ but $\delta^{34}\text{S}$ was significantly greater at non-vent sites ($p < 0.05$, Table 4; Fig. 4).
348 Variability was higher in vent sediments for all isotopic signatures. Faunal isotopic signatures
349 for $\delta^{13}\text{C}$ and $\delta^{34}\text{S}$ ranged much more widely than sediment signatures and indicate that sediment
350 organics were a mixture of two or more sources of organic matter. A few macrofaunal species
351 had relatively heavy $\delta^{13}\text{C}$ signatures that exceeded -20 ‰ that suggested either a heavy source
352 of carbon or marine carbonate in residual exoskeletal tissue, particularly for peracarids (~0 ‰).



353 Samples of pelagic salps from Hook Ridge had mean values for $\delta^{13}\text{C}$ of -27.4‰ (± 0.9) and $\delta^{34}\text{S}$
354 of 21.5‰ (± 0.8).

355

356 3.4. Comparing macrofaunal morphology and stable isotopic signatures

357

358 Averaged species isotopic data were each assigned to one of four clusters (SIMPROF, $p = 0.05$;
359 Supplementary Figure 3). No significant correlation between a-priori (based on morphology)
360 and a-posteriori clusters (based on isotopic data) was detected (Spearman Correlation Test: $Z =$
361 -1.34 ; $N = 43$; $p = 0.18$). Clusters were mainly discriminated based on $\delta^{15}\text{N}$ values and peracarids
362 were the only taxa to be represented in all of the clusters, indicating high trophic diversity.

363

364 Several taxa found at both vent and non-vent sites were assigned to different clusters between
365 sites. A total of eleven taxa were sampled from both vent and non-vent regions, of which four
366 were assigned to different clusters at vent and non-vent sites. Neotanaids (Peracarida:
367 Tanaidacea) had the greatest Euclidean distance between vent/ non-vent samples (11.36),
368 demonstrating clear differences in dietary composition (Fig. 5). All other species were separated
369 by much smaller distances between regions (range: 0.24 to 2.69). Raw $\delta^{13}\text{C}$ and $\delta^{15}\text{N}$ values were
370 also compared between vent and non-vent samples for each species (one-way ANOVA with
371 Tukey HSD pairwise comparisons). Analysis of the raw data indicated that $\delta^{13}\text{C}$ signatures were
372 different for neotanaids only and $\delta^{15}\text{N}$ were different for neotanaids and an oligochaete species
373 (*Limnodriloides* sp.) (ANOVA, $p < 0.01$, Fig. 5).

374

375 3.5. Community-level trophic metrics

376



377 All site niches overlapped (mean = 50 %, range = 30 – 82 %) and the positions of ellipse centroids
378 were broadly similar for all sites (Table 5; Fig 6). Vent site ellipse areas were similar but
379 significantly smaller than non-vent ellipses (SEA.B, $n = 10^5$, $p = < 0.05$). There were no significant
380 differences in ellipse area between any of the non-vent sites. Ranges in carbon sources (dCr)
381 were higher for non-vent sites (Table 5) indicating a greater trophic diversity in background
382 conditions. Nitrogen range (dNr, Table 5) was similar between vents and non-vents suggesting
383 a similar number of trophic levels within each assemblage. All site ellipses had broadly similar
384 eccentricity (degree of extension along long axis), ranging 0.85 – 0.97 (Table 5), however theta
385 (angle of long axis) differed between vent and non-vent sites (-1.43 to 1.55 at Hook Ridge, 0.67
386 to 0.86 at non-vent sites). Range in nitrogen sources was more influential at vent sites as
387 *Sclerolinum contortum*, which had very low $\delta^{15}\text{N}$ signatures but similar $\delta^{13}\text{C}$ values, when
388 compared with non-endosymbiont bearing taxa from the same sites. The strongly depleted $\delta^{13}\text{C}$
389 measurements of *Siboglinum* sp. meant that ellipse theta was skewed more towards horizontal
390 (closer to zero) for non-vent sites.

391



392 Section 4. Discussion

393

394 4.1. Microbial signatures of hydrothermal activity

395

396 PLFA profiles between the off-axis site and the Three Sisters indicated similar bacterial biomass
397 at each of these non-vent sites and that bacterial biomass varied much more widely at Hook
398 Ridge (Table 3). The Hook Ridge 2 sample is not directly comparable to the others as it was
399 sampled from sediment 0 – 2 cmbsf (owing to sample mass availability), though organic carbon
400 content, hydrogen sulphide flux and taxonomic diversity were all lower at this site and may
401 support suggestion of a lower overall bacterial biomass (Aquilina et al. 2013, Bell et al. 2016b).
402 The very high bacterial biomass at Hook Ridge 1 suggests a potentially very active bacterial
403 community, comparable to other hydrothermal sediments (Yamanaka & Sakata 2004) but
404 $\delta^{13}\text{C}_{\text{org}}$ was qualitatively similar to non-vent sites, implying that chemosynthetic activity was
405 comparatively limited, or that the isotopic signatures of the basal carbon source (e.g. DIC) and
406 the fractionation associated with FA synthesis resulted in similar $\delta^{13}\text{C}$ signatures.

407

408 Hook Ridge 1 PLFA composition was intermediate between non-vent sites and Hook Ridge 2
409 (Supplementary Fig. 2) but the PLFA suite was quite similar between Hook Ridge 1 and the off-
410 axis site (Fig. 2). A small number of the more abundant PLFAs had notable differences in relative
411 abundance between vent/ non-vent sites (Table 3). For example, 16:1 ω 7, which has been linked
412 to sulphur cycling pathways (Colaço et al. 2007) comprised 14.0 % – 15.2 % of abundance at
413 non-vent sites and 20.0 % – 23.5 % at vent sites. However, 18:1 ω 7, also a suggested PLFA linked
414 to thio-oxidation (McCaffrey et al. 1989, Colaço et al. 2007) occurred in lower abundance at vent
415 sites (4.8 % – 11.1 %) than non-vent sites (15.9 % – 16.9 %), and was also abundant in deeper
416 areas of the Antarctic shelf (Würzberg et al. 2011). These results further suggest that



417 chemosynthetic activity was relatively limited since, although there were differences between
418 sites in PLFAs that are potentially indicative of chemosynthetic activity, these were not
419 necessarily consistent between different PLFAs. The metabolic provenance of several of the
420 more abundant PLFAs is also still uncertain. A number of fatty acids have been linked, though
421 not exclusively, to chemoautotrophy, such as 10-Me-16:0 (*Desulfobacter* or *Desulfocurvus*,
422 Sulphate reducers) and 18:1 ω 7 (Yamanaka & Sakata 2004, Colaço et al. 2007, Klouche et al. 2009,
423 Boschker et al. 2014) and the presence of these FAs may be consistent with the hydrothermal
424 signature of the sediment microbial community. Together C16:1 ω 7c and C18:1 ω 7 accounted for
425 ~25-35% of the total PLFA suite. While they can be more generally associated with gram-
426 negative eubacteria, these PLFAs in sediment samples have frequently been linked to sulphur
427 oxidising bacteria (Pond et al. 1998, Yamanaka & Sakata 2004, Boschker et al. 2014). Their
428 dominance of the suite in the Bransfield Strait is similar to sediments from a vent in the Barbados
429 Trench, where together C16:1 ω 7 and C18:1 ω 7 contributed up to 50% of PLFAs (Guezennec &
430 Fiala-Medioni 1996). They have also been shown to be dominant in the PLFA suites of sulphur
431 oxidising bacteria such as *Beggiatoa* (e.g. Guezennec et al. 1998). The PLFA suites also contained
432 notable proportions of compounds normally associated with sulphate reducing bacteria
433 (Kohring et al. 1994, Boschker et al. 2014). These included iC15:0, aiC15:0, 1C17:0 and aiC17:0,
434 which together constituted ~8-12 % of the PLFA suite. In addition, C16:1 ω 5c was relatively
435 abundant (Supplementary figure 1), and minor amounts of 10MeC16:0, C17:1 ω 8c, and
436 cycloC17:0 were present. These have also been used as indicators of sulphate reducing bacteria,
437 and sometimes of particular groups (e.g. Guezennec & Fiala-Medioni 1996, Boschker et al. 2014).
438 These compounds indicate the presence of sulphate reducing bacteria, although perhaps not as
439 the dominant group. Although the PLFA suite was indicative of active sulphur cycling activity, it
440 remains difficult to be conclusive about the origin of most PLFAs even those which have been



441 regularly observed in chemosynthetic contexts (e.g. 18:1 ω 7) may still be abundant elsewhere
442 (Würzberg et al. 2011).

443

444 Unsurprisingly, long chain fatty acids (>C22) indicative of land plants (e.g. Yamanaka & Sakata
445 2004) were negligible or absent. More notably, the typical indicators of marine phytoplankton
446 production C20:3 ω 5 and C22:6 ω 3 were very minor constituents, never accounting for more
447 than 3% of PLFAs and only detected at the non-vent sites Off Vent and Middle Sister. While their
448 low abundance is at least partially accounted for by rapid degradation of polyunsaturated fatty
449 acids during sinking through the water column (Veuger et al. 2012), it also suggests that
450 sedimentary PLFAs are dominantly of bacterial origin, whether that be due to bacterial
451 reworking of photosynthetic organic matter, or in situ production, and that this influence of
452 bacterial activity is greater at vent sites than at non-vent sites.

453

454 Heavier carbon isotopic signatures (> -15 ‰) are generally associated with rTCA cycle carbon
455 fixation (Hayes 2001, Hugler & Sievert 2011, Reid et al. 2013), suggesting that this pathway may
456 have been active at the vent sites, albeit at probably quite low rates. Conversely, many of the
457 lightest $\delta^{13}\text{C}$ signatures (e.g. 19:1 ω 8, -56.6 ‰, off-axis site) were associated with the non-vent
458 sites, however 19:1 ω 8 has not been directly associated with a particular bacterial process
459 (Koranda et al. 2013, Dong et al. 2015). Lower PLFA carbon isotope signatures with small ranges
460 (e.g. -60 ‰ to -50 ‰) could also be indicative of methane cycling, but most PLFAs at all sites
461 had $\delta^{13}\text{C}$ of > -40 ‰.

462

463 Several PLFAs had isotopic signatures that varied widely between sites, demonstrating
464 differences in fractionation and/ or source isotopic signatures. Fang et al. (2006) demonstrated
465 that depth (i.e. pressure) can exert an influence upon PLFA fractionation, but at these sites, depth



466 varied only by a small amount (1045 – 1312 m), meaning that this effect should have been quite
467 limited. The heaviest PLFA $\delta^{13}\text{C}$ signatures were associated with Hook Ridge sites (e.g. 16:1 ω 11t
468 at HR2, $\delta^{13}\text{C}$ = -8.7 ‰, ~-24 ‰ to -25 ‰ elsewhere). This suggests isotopic differences in the
469 sources or fractionation by the metabolic pathways used to synthesise these FAs. However,
470 bacterial fractionation of organic matter can have substantial variation in $\delta^{13}\text{C}$ signatures,
471 depending upon variability in the composition and quality (e.g. C: N ratios) of the source (Macko
472 & Estep 1984) and growth of the organism (Fang et al. 2006), which makes it difficult to elucidate
473 the specific nature of the differences in substrates between sites.

474

475 *Siboglinum* isotopic data demonstrates that methanotrophy was probably occurring at the off
476 axis sites (Supplementary Figure 1), and depleted PLFA isotopic signatures (e.g. 19:1 ω 8 - $\delta^{13}\text{C}$: -
477 56.6 ‰; Table 3) provide further suggestion of methanotrophy amongst free-living sedimentary
478 bacteria. Chemotrophic bacterial sequences, such as *Blastopirellula* (Schlesner 2015) or
479 *Rhodopirellula* (Bondoso et al. 2014) were found at all sites in relatively high abundance,
480 suggesting widespread and active chemosynthesis, though the lack of a particularly dominant
481 bacterial group associated with chemosynthetic activity suggested that the supply of
482 chemosynthetic OM was likely relatively limited. It remains difficult however to determine
483 which PLFAs these bacterial lineages may be have been synthesising.

484

485 Some PLFAs also had marked differences in $\delta^{13}\text{C}$ signatures, even where there was strong
486 compositional similarity between sites (i.e. the non-vent sites). This suggested that either there
487 were differences in the isotopic values of inorganic or organic matter sources or different
488 bacterial metabolic pathways were active. Between the non-vent sites, these PLFAs included
489 PUFAs and MUFAs (Poly- and Mono-unsaturated fatty acids) such as 18:2 ω 6, 9 ($\Delta\delta^{13}\text{C}$ 24.4 ‰)
490 and 19:1 ω 8 ($\Delta\delta^{13}\text{C}$ 19.1 ‰). Differences in PLFA $\delta^{13}\text{C}$ between Hook Ridge sites also ranged



491 widely, with the largest differences being associated with PLFAs such as 16:1 ω 11t ($\Delta\delta^{13}\text{C}$
492 17.2 ‰) and 10-Me-16:0 ($\Delta\delta^{13}\text{C}$ 11.0 ‰). However, it should be stressed that all PLFAs with
493 larger $\delta^{13}\text{C}$ differences between sites were comparatively rare and never individually exceeded
494 5% of total abundance. This provides further evidence of limited chemosynthetic activity at all
495 sites and is consistent with the presence of bacteria associated with methane and sulphur cycling.
496 Microbial signatures, whilst supporting the suggestion of chemosynthetic activity, are not
497 indicative of chemosynthetic OM being the dominant source of organic matter to food webs at
498 any site (hypothesis four). It is not possible to assess from PLFA data the relative importance of
499 chemoautotrophic and photosynthetic OM sources, since PLFAs degrade quickly and therefore
500 surface FA abundances are inevitably underestimated in deep water samples. Abundance of
501 PLFAs associated with surface production, such as 15:0, 20:5 ω 3, C22: ω 6 (Colaço et al. 2007,
502 Parrish 2013) were low (max 1.8 %), which is consistent with the expected degradation rates
503 during sinking. Further, piezophilic bacteria have been shown to synthesise some long chain
504 PUFAs (20:5 ω 3 and 22:6 ω 3), which were previously thought to be algal markers (Fang et al.
505 2006).

506

507 4.2. Siboglinids

508

509 Both species of siboglinid (*Sclerolinum contortum* from Hook Ridge and *Siboglinum* sp. from the
510 non-vent sites) appeared to subsist upon chemosynthetically derived organic matter, as
511 evidenced by their morphology, and also by their strongly ^{15}N -depleted isotopic signatures (see
512 values with $\delta^{15}\text{N}$ of < -2 ‰ in Fig. 3). Low $\delta^{15}\text{N}$ signatures have also been observed in other
513 siboglinids in a range of hydrothermal settings, such as *Riftia pachyptila* at the East Pacific Rise
514 hard substratum vents (Rau 1981). Diazotrophy has been detected previously in hydrothermal
515 vents and cold seeps, and has been associated with low $\delta^{15}\text{N}$ values (e.g. Rau, 1981; Desai et al.,



516 2013; Wu et al., 2014 (Yamanaka et al. 2015). Diazotrophy in various reducing settings has been
517 found associated with anaerobic oxidation of methane (Dekas et al., 2009), methanotrophy
518 (Mehta & Baross 2006) and (in a non-marine cave) sulphate reduction (Desai et al. 2013) The
519 latter is also consistent with the low $\delta^{34}\text{S}$ signatures of both siboglinid species (Fig. 3; 4), but
520 gene expression analysis and/or isotopic tracing would be required to confirm this suggestion.
521 The low $\delta^{34}\text{S}$ may also be explained by assimilation of bacterial sulphide, which also gave rise to
522 metal sulphides (e.g. pyrite) at the vent sites (Petersen et al. 2004). Alternately, low $\delta^{15}\text{N}$
523 signatures may be explained by endosymbionts conducting dissimilatory nitrate reduction to
524 ammonium (Naraoka et al. 2008, Liao et al. 2014, Bennett et al. 2015), or strong isotopic
525 fractionation during utilization of ammonia (Naraoka et al. 2008, Liao et al. 2014, Bennett et al.
526 2015). Bulk faunal isotopic signatures are inadequate to determine which of these
527 chemosynthesis-related mechanisms is responsible for *Siboglinum* $\delta^{15}\text{N}$ values, which would
528 require analysis of the functional genes in the *Siboglinum* endosymbionts.

529

530 Whichever pathway is dominant, $\delta^{15}\text{N}$ values for both species ($\delta^{15}\text{N}$ *Sclerolinum* = $-5.3 \text{‰} \pm 1.0$,
531 *Siboglinum* = $-8.9 \text{‰} \pm 0.8$) seem to indicate reliance upon locally fixed N_2 (Rau 1981, Dekas et
532 al. 2009, Dekas et al. 2014, Wu et al. 2014, Yamanaka et al. 2015), rather than utilisation of
533 organic nitrogen sources within the sediment ($\delta^{15}\text{N}$ = $5.7 \text{‰} \pm 0.7$). These values were also in
534 contrast to the rest of the non-chemosynthetic obligate species, which generally had much
535 heavier $\delta^{15}\text{N}$ values. This supports hypothesis three, that the siboglinid species were subsisting
536 upon chemosynthetic OM, most likely supplied by their endosymbionts.

537

538 Carbon isotopic signatures in chemosynthetic primary production depend upon the mode of
539 fixation and the initial ^{13}C of available DIC. *Sclerolinum contortum* $\delta^{13}\text{C}$ ($-20.5 \text{‰} \pm 1.0 \text{‰}$) was
540 depleted in $\delta^{13}\text{C}$ relative to Southern Ocean DIC by around 10‰ (Henley et al. 2012, Young et



541 al. 2013), giving it a signal within the fractionation range of the reverse tricarboxylic acid cycle
542 (Yorisue et al. 2012). Regional measurements of surface ocean DIC $\delta^{13}\text{C}$ have an average isotopic
543 signature of -10.4‰ (Henley et al. 2012, Young et al. 2013) but the concentration and isotopic
544 composition of DIC can undergo considerable alteration at sedimented vents (Walker et al.
545 2008). Therefore, without measurements of $\delta^{13}\text{C}$ in pore fluid DIC, it was not possible to
546 determine which fixation pathway(s) were being used by *S. contortum* endosymbionts.

547

548 Sulphur isotopic signatures in *S. contortum* were very low, and quite variable ($-26.7\text{‰} \pm 3.5\text{‰}$).
549 *Sclerolinum* endosymbionts may have been utilising sulphide re-dissolved from hydrothermal
550 precipitates. Mineral sulphide was present at Hook Ridge that ranged between -28.1‰ to
551 $+5.1\text{‰}$ (Petersen et al. 2004), consistent with the relatively high $\delta^{34}\text{S}$ variability in *S. contortum*
552 (but $\delta^{34}\text{S}$ measurements were subject to higher error between replicates of standards). These
553 precipitates at Hook Ridge are thought to originate from a previous period of high-temperature
554 venting at this site (Klinkhammer et al. 2001). Alternatively, sulphide supplied as a result of
555 microbial sulphate reduction (Canfield 2001) may have been the primary source of organic
556 sulphur, similar to that of solemyid bivalves from reducing sediments near a sewage pipe outfall
557 (mean $\delta^{34}\text{S}$ ranged -30‰ to -20‰ ; Vetter and Fry (1998) and in cold seep settings (Yamanaka
558 et al. 2015). Sulphate reduction can also be associated with anaerobic oxidation of methane
559 (Whiticar & Suess 1990, Canfield 2001, Dowell et al. 2016), suggesting that methanotrophic
560 pathways could also have been important at Hook Ridge. (e.g. abundance of *Methylohalomonas*,
561 2.1% – 4.3% of sequences at all sites). Although endosymbiont composition data were not
562 available for the Southern Ocean population, *Sclerolinum contortum* is also known from
563 hydrocarbon seeps in the Gulf of Mexico (Eichinger et al. 2013, Eichinger et al. 2014, Georgieva
564 et al. 2015) and the Håkon Mosby mud volcano in the Arctic ocean, where *S. contortum* $\delta^{13}\text{C}$
565 ranged between -48.3‰ to -34.9‰ (Gebruk et al. 2003) demonstrating that this species is



566 capable of occupying several reducing environments and using a range of chemosynthetic
567 fixation pathways, including sulphide oxidation and methanotrophy (Eichinger et al. 2014,
568 Georgieva et al. 2015).

569

570 *Siboglinum* sp. $\delta^{13}\text{C}$ values (mean -41.4‰ , range -45.7‰ to -38.1‰ , $n = 8$) corresponded very
571 closely to published values of thermogenic methane (-43‰ to -38‰) from the Bransfield Strait
572 (Whiticar & Suess 1990). This suggested that methanotrophy was the likely carbon source for
573 this species. Biogenic methane typically has much lower $\delta^{13}\text{C}$ values (Whiticar 1999, Yamanaka
574 et al. 2015), indicating a hydrothermal/ thermogenic source of methane in the Bransfield Strait
575 (Whiticar & Suess 1990). Sources of microbially-mediated methane were also present in the
576 Bransfield Strait (Whiticar & Suess 1990) but these $\delta^{13}\text{C}$ values were far lower than any of the
577 faunal signatures observed here. Sulphur isotopic signatures were also very low in *Siboglinum*
578 sp. ($\delta^{34}\text{S}$ -22.9‰ , one sample from 15 pooled individuals from the off-axis site), the lowest
579 measurement of $\delta^{34}\text{S}$ reported for this genus (Schmaljohann & Flügel 1987, Rodrigues et al.
580 2013). The low $\delta^{13}\text{C}$, $\delta^{15}\text{N}$ and $\delta^{34}\text{S}$ signatures of *Siboglinum* sp. suggest that its symbionts may
581 have included methanotrophs (Thornhill et al. 2008) and diazotrophic/ denitrifying bacteria
582 (Boetius et al. 2000, Canfield 2001, Dekas et al. 2009). Methanotrophy in *Siboglinum* spp. has
583 been previously documented at seeps in the NE Pacific (Bernardino & Smith 2010) and
584 Norwegian margin ($\delta^{13}\text{C} = -78.3\text{‰}$ to -62.2‰) (Schmaljohann et al. 1990) and in Atlantic mud
585 volcanoes ($\delta^{13}\text{C}$ range -49.8‰ to -33.0‰) (Rodrigues et al. 2013). Sulphur isotopic signatures
586 in *Siboglinum* spp. from Atlantic mud volcanoes ranged between -16.8‰ to 6.5‰ (Rodrigues
587 et al. 2013) with the lowest value still being 6‰ greater than that of Bransfield strait specimens.
588 Rodrigues et al. (2013) also reported a greater range in $\delta^{15}\text{N}$ than observed in the Bransfield
589 siboglinids ($\delta^{15}\text{N}$ -1.3‰ to 12.2‰ and -10.2‰ to -7.6‰ respectively). This suggests that, in
590 comparison to *Siboglinum* spp. in Atlantic Mud volcanoes, which seemed to be using a mixture



591 of organic matter sources (Rodrigues et al. 2013), the Bransfield specimens relied much more
592 heavily upon a single OM source, suggesting considerable trophic plasticity in this genus
593 worldwide.

594

595 Off-vent methanotrophy, using thermogenic methane, potentially illustrates an indirect
596 dependence upon hydrothermalism (Whiticar & Suess 1990). Sediment methane production is
597 thought to be accelerated by the heat flux associated with mixing of hydrothermal fluid in
598 sediment (Whiticar & Suess 1990) and sediment and *Siboglinum* isotopic data suggest that the
599 footprint of hydrothermal influence may be much larger than previously recognised, giving rise
600 to transitional environments (Bell et al. 2016a, Levin et al. 2016). Clear contribution of methane-
601 derived carbon to consumer diets was limited predominately to neotanaids, consistent with the
602 relatively small population sizes (64 ind. m⁻²– 159 ind. m²) of *Siboglinum* sp. observed in the
603 Bransfield Strait (Bell et al. 2016b).

604

605 4.3. Organic Matter Sources

606

607 Pelagic salps, collected from an Agassiz trawl at Hook Ridge (1647m), were presumed to most
608 closely represent a diet of entirely surface-derived material and were more depleted in ¹³C and
609 more enriched in ³⁴S than were sediments (Salp $\delta^{13}\text{C} = -27.4 \text{ ‰}$ & $\delta^{34}\text{S} = 20.1$; Hook Ridge
610 sediment $\delta^{13}\text{C} = -26.2 \text{ ‰}$ & $\delta^{34}\text{S} = 14.3$) Salp samples were also lighter than the majority of
611 macrofauna, both at Hook Ridge and the non-vent sites (Fig. 3) and similar to other suspension
612 feeding fauna in the Bransfield Strait (Elias-Piera et al. 2013).

613

614 Sediment bulk organic C ($\delta^{13}\text{C} -25.8$ to -26.2) was similar to but nonetheless isotopically heavier
615 than the salp samples. Sediment PLFA data shows that 20.8 - 29.9 % were attributed to bacteria



616 (summed contributions of $i15:0$, $ai15:0$, $16:1\omega5c$, $i17:0$, $ai17:0$, $17:0$, and $18:1\omega7$; Parrish
617 (2013)), while only 1.0 - 3.8 % were indicative of algal inputs (summed contributions of $15:0$,
618 $20:5\omega3$, $22:6\omega3$; Parrish (2013)). Thus, while the C isotopes suggest that sedimentary OM was
619 dominantly derived from surface photosynthesis, the material deposited in the sediment was
620 likely strongly reworked by bacterial activity.

621

622 This suggests that fauna with more depleted $\delta^{34}S$ / more enriched $\delta^{13}C$ values are likely to have
623 derived at least a small amount of their diet from chemosynthetic sources (potentially indirectly
624 through non-selective consumption of detrital OM), both at vents and background regions.
625 Carbon and sulphur isotopic measurements indicated mixed sources for most consumers
626 between chemosynthetic OM and surface-derived photosynthetic OM. Sediment OM was likely a
627 combination of these two sources, making both available to non-specific deposit-feeding fauna
628 and suggesting that consumption of chemosynthetic OM may even have been incidental in some
629 cases. The low content of algal biomarkers (particularly at the vent sites) suggests that
630 phytodetritus was probably quite degraded and thus challenging to detect using short-lived fatty
631 acids. However, the Bransfield Strait can be subject to substantial export production and it is
632 probable that surface production contributes much more to seafloor OM than is evident from
633 the fatty acid composition. Non-vent sediments were more enriched in ^{34}S than vent sediments,
634 an offset that probably resulted from greater availability of lighter sulphur sources such as
635 sulphide oxidation at Hook Ridge.

636

637 Samples of bacterial mat could not be collected during JC55 (Tyler et al. 2011) and without these
638 endmember measurements, it was not possible to quantitatively model resource partitioning in
639 the Bransfield Strait using isotope mixing models (Phillips et al. 2014). Bacterial mats from high-
640 temperature vents in the Southern Ocean had $\delta^{34}S$ values of 0.8 ‰ (Reid et al. 2013) and at



641 sedimented areas of the Loki's Castle hydrothermal vents in the Arctic Ocean has $\delta^{34}\text{S}$ values of
642 -4.9‰ (Bulk sediment; Jaeschke et al. 2014). Therefore it is probable that low faunal $\delta^{34}\text{S}$ values
643 represent a contribution of chemosynthetic OM (from either siboglinid tissue or free-living
644 bacteria). Inorganic sulphur can also be a source to consumers when sulphide is utilised by free
645 living bacteria ($\delta^{34}\text{S}$ ranged -7.3‰ to 5.4‰ ; Erickson et al. (2009)) and, although we could not
646 analyse the $\delta^{34}\text{S}$ of fluid sulphide, sulphide crusts have been found at Hook Ridge and may
647 provide a proxy for typical isotopic composition ($\delta^{34}\text{S}$ -28.1‰ to 5.1‰ ; Petersen et al. (2004)).
648 There were several species (e.g. Tubificid oligochaetes) that had moderately depleted $\delta^{34}\text{S}$
649 signatures, such as *Limnodriloides* sp. ($\delta^{34}\text{S}$ 7.6‰ at vents, -1.2‰ at non-vents, Fig. 4) further
650 supporting the hypothesis of different trophic positions between vent/ non-vent regions
651 (hypothesis two). This provides evidence of coupled anaerobic oxidation of methane/ sulphate
652 reduction but overall, the contribution of $\delta^{34}\text{S}$ -depleted bacterial production did not seem
653 widespread (further rejecting hypothesis four).

654

655 Without samples of all OM sources we cannot quantitatively assert that faunal utilisation of
656 chemosynthetic OM was low in the Bransfield Strait. Although isotopic data were consistent with
657 several OM sources, it seemed unlikely that chemosynthetic OM was a dominant source of OM
658 to the vast majority of taxa. The apparently limited consumption of chemosynthetic OM
659 suggested that either it was not widely available (e.g. patchy or low density of endosymbiont-
660 bearing fauna (Bell et al. 2016b)), or that the ecological stress associated with feeding in areas
661 of in situ production was a significant deterrent to many species (Bernardino et al. 2012, Levin
662 et al. 2013).

663

664 4.4. A-priori vs. a-posteriori trophic groups

665



666 Morphology did not prove to be an accurate predictor of trophic associations, suggesting that
667 faunal behaviour is potentially more important in determining dietary composition than
668 morphology (e.g. having/ lacking jaws). Peracarid species that possessed structures adapted to
669 a motile, carnivorous lifestyle were assigned to a carnivore/ scavenger guild (Bell et al. 2016b)
670 and were distributed throughout the food web both at vents and background regions, indicating
671 more diverse feeding strategies than expected. Taxa presumed to be deposit feeders (largely
672 annelids) also had a surprisingly large range of $\delta^{15}\text{N}$ values. This may reflect the consumption of
673 detritus from both 'fresh' and more recycled/ refractory OM sources as observed in other non-
674 vent sedimented deep-sea habitats (Iken et al. 2001, Reid et al. 2012) or reflect variability in
675 trophic discrimination related to diet quality (Adams & Sterner 2000). Another possibility is taxa
676 feeding on foraminifera conducting denitrification. A range of foraminifera have now been
677 shown to conduct this process, which results in them showing elevated $\delta^{15}\text{N}$ leading to heavy
678 $\delta^{15}\text{N}$ values (Pina-Ochoa et al. 2010, Jeffreys et al. 2015). The result is high $\delta^{15}\text{N}$ values in taxa
679 without predatory morphology (e.g. oligochaetes) (Bell et al. 2016a). Tubificid oligochaetes had
680 higher $\delta^{15}\text{N}$ values at the vent sites, suggesting that they fed upon more recycled organic matter,
681 possibly owing to greater microbial activity at vent sites. Bacterial biomass was very variable at
682 the vent sites (86 mg C m^{-2} – 535 mg C m^{-2} , compared with 136 mg C m^{-2} – 197 mg C m^{-2} at non-
683 vent sites; Table 3) and so it is possible that at Hook Ridge 1 bacterial assemblages could have
684 had a greater influence upon $\delta^{15}\text{N}$ of organic matter.

685

686 Neotanaids from the off-axis site had the lowest $\delta^{13}\text{C}$ and $\delta^{15}\text{N}$ values of any non-siboglinid taxon
687 (Fig. 5), suggesting a significant contribution of methane-derived carbon. The clustering of the
688 neotanaids together with endosymbiont-bearing taxa is far more likely to be an artefact of the
689 cluster linkage method, introduced by consumption of low $\delta^{13}\text{C}$ methanotrophic sources (e.g.



690 *Siboglinum* tissue), rather than suggesting symbionts in these fauna (Larsen 2006, Levin et al.
691 2009).

692

693 Several taxa (e.g. neotanaiids from the off-axis site and ophiuroids at Hook Ridge) had low $\delta^{15}\text{N}$
694 values relative to sediment OM, suggesting preferential consumption of chemosynthetic OM
695 (Rau 1981, Dekas et al. 2014). In these taxa, it is likely that the widespread, but patchy bacterial
696 mats or *Sclerolinum* populations at Hook Ridge (Aquilina et al. 2013) were an important source
697 of organic matter to fauna with low $\delta^{15}\text{N}$ values (e.g. ophiuroids). Fauna from the non-vent sites
698 with low $\delta^{15}\text{N}$ were likely subsisting in part upon siboglinid tissue (*Siboglinum* sp.). There were
699 no video transects over the off-axis site but footage of the Three Sisters, which was similar in
700 macrofaunal composition (Bell et al. 2016b), did not reveal bacterial mats (Aquilina et al. 2013),
701 hence it is unlikely that these were an important resource at non-vent sites.

702

703 It is clear that some fauna can exhibit a degree of trophic plasticity, depending upon habitat
704 (supporting hypothesis two). This is consistent with other SHVs where several taxa (e.g.
705 *Prionospio* sp. – Polychaeta: Spionidae) had different isotopic signatures, depending upon their
706 environment (Levin et al. 2009), demonstrating differential patterns in resource utilisation.
707 Alternatively, there could have been different $\delta^{15}\text{N}$ baselines between sites, though if these
708 differences were significant, we argue that it likely that more species would have had significant
709 differences in tissue $\delta^{15}\text{N}$. Conversely, samples of *Aurospio foodbancsia* at both vent and non-
710 vent sites had broadly similar $\delta^{15}\text{N}$ values to that of the west Antarctic Peninsula; 8.1 ‰ and
711 7.9 ‰ respectively, albeit with a higher variability (Mincks et al. 2008). $\delta^{13}\text{C}$ values of *Aurospio*
712 were also broadly similar, implying that this species occupied a detritivorous trophic niche,
713 irrespective of environmental conditions.

714



715 4.5. Impact of hydrothermal activity on community trophodynamics

716

717 Standard ellipse area was lower at Hook Ridge than at non-vent sites (Table 5), analogous to
718 trends in macrofaunal diversity and abundance in the Bransfield Strait (Bell et al. 2016b) and
719 changes in SEA.B along a gradient of methane flux at vent and seep ecosystems in the Guaymas
720 Basin (Portail et al. 2016). This demonstrates that at community level, ellipse area can be
721 associated with other macrofaunal assemblage characteristics. This concurrent decline in niche
722 area and alpha diversity is consistent with the concept that species have finely partitioned niches
723 and greater total niche area permits higher biodiversity (McClain & Schlacher 2015).
724 Productivity-diversity relationships, whereby higher productivity sustains higher diversity,
725 have also been suggested for deep-sea ecosystems (McClain & Schlacher 2015, Woolley et al.
726 2016) but in the absence of measurements of in situ organic matter fixation rates at Hook Ridge,
727 it is unclear whether such relationships exist in the Bransfield Strait. Sediment organic carbon
728 content was similar between Hook Ridge 1 and non-vent sites but was slightly lower at Hook
729 Ridge 2 (Bell et al. 2016b), which is not consistent with variation in niche area. The decline in
730 alpha diversity and niche area is consistent with the influence of disturbance gradients created
731 by hydrothermalism that result in an impoverished community (McClain & Schlacher 2015, Bell
732 et al. 2016b). We suggest that, in the Bransfield Strait, the environmental toxicity at SHVs (from
733 differences in temperature and porewater chemistry) causes a concomitant decline in both
734 trophic and species diversity (Bell et al. 2016b), in spite of the potential for increased localised
735 production. However, we acknowledge that, owing to the high small-scale habitat heterogeneity
736 apparent from video imagery over the vent area, that it is likely that the contribution of
737 chemosynthetic organic matter varies widely over 10s of metres at Hook Ridge.

738



739 Community-based trophic metrics (Layman et al. 2007) indicated that, although measures of
740 dispersion within sites were relatively similar between vents and background areas (Table 5),
741 trophic diversity, particularly in terms of range of carbon sources (dCr) and total hull area (TA)
742 were higher at background sites. It was expected that trophic diversity would be greater at Hook
743 Ridge but the greater dCr at non-vent sites (owing to the methanotrophic source) meant that the
744 isotopic niches at these sites were larger. Range in nitrogen values (dNr) was also greater at non-
745 vents, driven by the more heavily depleted $\delta^{15}\text{N}$ values of *Siboglinum* sp. It is of course debatable
746 whether this assemblage isotopic niche really corresponds to the assemblage's actualised
747 trophic niche and, although the niche space was smaller at the vent sites, the potential for
748 different trophic strategies was still potentially greater than at non-vent sites. Differences in
749 eccentricity are more heavily influenced by the spread of all isotopes used to construct the niche
750 space (where $E = 0$ corresponds to an equal influence of both carbon and nitrogen) whereas
751 theta (the angle of the long axis) determines which, if any, isotope is most influential in
752 determining ellipse characteristics (Reid et al. 2016). For the non-vent sites, the dominant
753 isotope was carbon, owing to the relatively light $\delta^{13}\text{C}$ of methanotrophic source utilised by
754 *Siboglinum*. Some sites, particularly the Axe, had several fauna with heavy $\delta^{13}\text{C}$ values (Fig. 6),
755 which could be explained by either contamination from marine carbonate ($\sim 0\text{‰}$), as specimens
756 were not acidified, or a diet that included a heavier source of carbon, such as sea ice algae
757 (Henley et al. 2012).



758 Section 5. Conclusions

759

760 In this study, we demonstrate the influence of sediment-hosted hydrothermal venting upon
761 trophodynamics and microbial populations. Low activity vent microbiota were more similar to
762 the non-vent site than to high activity populations, illustrating the effect of ecological gradients
763 upon deep-sea microbial diversity. Despite widespread bacterial mats, and populations of vent-
764 endemic macrofauna, utilisation of chemosynthetic OM amongst non-specialist macro- and
765 megafauna seemed relatively low, with a concomitant decline in trophic diversity with
766 increasing hydrothermal activity. Morphology was also not indicative of trophic relationships,
767 demonstrating the effects of differential resource availability and behaviour. We suggest that,
768 because these sedimented hydrothermal vents are insufficiently active to host large populations
769 of vent-endemic megafauna, the transfer of chemosynthetic organic matter into the metazoan
770 food web is likely to be more limited than in other similar environments.



771 6. Acknowledgements

772

773 JBB was funded by a NERC PhD Studentship (NE/L501542/1). This work was funded by the
774 NERC ChEsSo consortium (Chemosynthetically-driven Ecosystems South of the Polar Front,
775 NERC Grant NE/DOI249X/I). Elemental analyses were funded by the NERC Life Sciences Mass
776 Spectrometry Facility (Proposal no. EK234-13/14). We thank Barry Thornton and the James
777 Hutton Laboratory, Aberdeen for processing the PLFA samples. We also thank Will Goodall-
778 Copestake for assistance in processing the 16S sequence data. We are grateful to the Master and
779 Crew of RRS *James Cook* cruise 055 for technical support and the Cruise Principal Scientific
780 Officer Professor Paul Tyler.

781

782 7. Ethics Statement

783

784 In accordance with the Antarctic Act (1994) and the Antarctic Regulations (1995), necessary
785 permits (S5-4/2010) were acquired from the South Georgia and South Sandwich Islands
786 Government.

787

788 8. Author contributions

789

790 Conceived and designed the sampling programme: WDKR, DAP, AGG, CJS & CW. Sample
791 laboratory preparation and isotopic analyses: JBB, JN & CJS. Microbial sequencing: DAP.
792 Statistical analyses: JBB. Produced figures: JBB. Wrote the paper: JBB, CW & WDKR, with
793 contributions and comments from all other authors.



794 9. References

795

- 796 Adams TS, Sterner RW (2000) The effect of dietary nitrogen content on trophic level ¹⁵N
797 enrichment. *Limnology & Oceanography* 45:601-607
- 798 Aquilina A, Connelly DP, Copley JT, Green DR, Hawkes JA, Hepburn L, Huvenne VA, Marsh L, Mills
799 RA, Tyler PA (2013) Geochemical and Visual Indicators of Hydrothermal Fluid Flow
800 through a Sediment-Hosted Volcanic Ridge in the Central Bransfield Basin (Antarctica).
801 *Plos One* 8:e54686
- 802 Aquilina A, Homoky WB, Hawkes JA, Lyons TW, Mills RA (2014) Hydrothermal sediments are a
803 source of water column Fe and Mn in the Bransfield Strait, Antarctica. *Geochimica et*
804 *Cosmochimica Acta* 137:64-80
- 805 Bell JB, Aquilina A, Woulds C, Glover AG, Little CTS, Reid WDK, Hepburn LE, Newton J, Mills RA
806 (2016a) Geochemistry, faunal composition and trophic structure at an area of weak
807 methane seepage on the southwest South Georgia margin. *Royal Society Open Science* 3
- 808 Bell JB, Woulds C, Brown LE, Little CTS, Sweeting CJ, Reid WDK, Glover AG (2016b) Macrofaunal
809 ecology of sedimented hydrothermal vents in the Bransfield Strait, Antarctica. *Frontiers*
810 *in Marine Science* 3:32
- 811 Bemis K, Lowell R, Farough A (2012) Diffuse Flow On and Around Hydrothermal Vents at Mid-
812 Ocean Ridges. *Oceanography* 25:182-191
- 813 Bennett SA, Dover CV, Breier JA, Coleman M (2015) Effect of depth and vent fluid composition
814 on the carbon sources at two neighboring deep-sea hydrothermal vent fields (Mid-
815 Cayman Rise). *Deep Sea Research Part I: Oceanographic Research Papers* 104:122-133
- 816 Bernardino AF, Levin LA, Thurber AR, Smith CR (2012) Comparative Composition, Diversity and
817 Trophic Ecology of Sediment Macrofauna at Vents, Seeps and Organic Falls. *Plos ONE*
818 7:e33515
- 819 Bernardino AF, Smith CR (2010) Community structure of infaunal macrobenthos around
820 vestimentiferan thickets at the San Clemente cold seep, NE Pacific. *Marine Ecology-an*
821 *Evolutionary Perspective* 31:608-621
- 822 Biomatters (2014) Geneious.
- 823 Bligh EG (1959) A rapid method of total lipid extraction and purification. *Canadian Journal of*
824 *Biochemistry and Physiology* 37:911-917
- 825 Boetius A, Ravensschlag K, Schubert CJ, Rickert D, Widdel F, Gieseke A, Amman R, Jørgensen BB,
826 Witte U, Pfannkuche O (2000) A marine microbial consortium apparently mediating
827 anaerobic oxidation of methane. *Nature* 407:623-626
- 828 Bondoso J, Albuquerque L, Lobo-da-Cunha A, da Costa MS, Harder J, Lage OM (2014)
829 *Rhodopirellula lusitana* sp. nov. and *Rhodopirellula rubra* sp. nov., isolated from the
830 surface of macroalgae. *Syst Appl Microbiol* 37:157-164
- 831 Boschker HT, Middelburg JJ (2002) Stable isotopes and biomarkers in microbial ecology. *FEMS*
832 *Microbiology Ecology* 40:85-95
- 833 Boschker HT, Vasquez-Cardenas D, Bolhuis H, Moerdijk-Poortvliet TW, Moodley L (2014)
834 Chemoautotrophic carbon fixation rates and active bacterial communities in intertidal
835 marine sediments. *PLoS One* 9:e101443
- 836 Canfield DE (2001) Isotope fractionation by natural populations of sulfate-reducing bacteria.
837 *Geochimica Et Cosmochimica Acta* 65:1117-1124
- 838 Clarke KR, Somerfield PJ, Gorley RN (2008) Testing of null hypotheses in exploratory community
839 analyses: similarity profiles and biota-environment linkage. *Journal of Experimental*
840 *Marine Biology and Ecology* 366:56-69



- 841 Colaço A, Desbruyères D, Guezennec J (2007) Polar lipid fatty acids as indicators of trophic
842 associations in a deep-sea vent system community. *Marine Ecology* 28:15-24
- 843 Connolly RM, Schlacher TA (2013) Sample acidification significantly alters stable isotope ratios
844 of sulfur in aquatic plants and animals. *Marine Ecology Progress Series* 493:1-8
- 845 Dählmann A, Wallman K, Sahling H, Sarthou G, Bohrmann G, Petersen S, Chin CS, Klinkhammer
846 GP (2001) Hot vents in an ice-cold ocean: Indications for phase separation at the
847 southernmost area of hydrothermal activity, Bransfield Strait, Antarctica. *Earth and
848 Planetary Science Letters* 193:381-394
- 849 Dekas AE, Chadwick GL, Bowles MW, Joye SB, Orphan VJ (2014) Spatial distribution of nitrogen
850 fixation in methane seep sediment and the role of the ANME archaea. *Environ Microbiol*
851 16:3012-3029
- 852 Dekas AE, Poretsky RS, Orphan VJ (2009) Deep-sea archaea fix and share nitrogen in methane-
853 consuming microbial consortia. *Science* 326:422-426
- 854 Desai MS, Assig K, Dattagupta S (2013) Nitrogen fixation in distinct microbial niches within a
855 chemoautotrophy-driven cave ecosystem. *Isme Journal* 7:2411-2423
- 856 Dong L-J, Sun Z-K, Gao Y, He W-M (2015) Two-year interactions between invasive *Solidago*
857 *canadensis* and soil decrease its subsequent growth and competitive ability. *Journal of
858 Plant Ecology*:rtv003
- 859 Dowell F, Cardman Z, Dasarathy S, Kellerman M, Lipp JS, Ruff SE, Biddle JF, McKay L, MacGregor
860 BJ, Lloyd KG, Albert DB, Mendlovitz H, Hinrichs KU, Teske A (2016) Microbial
861 communities in methane- and short chain alkane- rich hydrothermal sediments of
862 Guaymas Basin. *Frontiers in microbiology*
- 863 Eichinger I, Hourdez S, Bright M (2013) Morphology, microanatomy and sequence data of
864 *Sclerolinum contortum* (Siboglinidae, Annelida) of the Gulf of Mexico. *Organisms Diversity
865 & Evolution* 13:311-329
- 866 Eichinger I, Schmitz-Esser S, Schmid M, Fisher CR, Bright M (2014) Symbiont-driven sulfur
867 crystal formation in a thiotrophic symbiosis from deep-sea hydrocarbon seeps. *Environ
868 Microbiol Rep* 6:364-372
- 869 Elias-Piera F, Rossi S, Gili JM, Orejas C (2013) Trophic ecology of seven Antarctic gorgonian
870 species. *Marine Ecology Progress Series* 477:93-106
- 871 Erickson KL, Macko SA, Van Dover CL (2009) Evidence for a chemotrophically based food web
872 in inactive hydrothermal vents (Manus Basin). *Deep Sea Research Part II: Topical Studies
873 in Oceanography* 56:1577-1585
- 874 Fanelli E, Cartes JE, Enric J, Papiol V, Rumolo P, Sprovieri M (2010) Effects of preservation on the
875 $\delta^{13}\text{C}$ and $\delta^{15}\text{N}$ values of deep sea macrofauna. *Journal of Experimental Marine Biology
876 and Ecology* 395:93-97
- 877 Fang J, Uhle M, Bilimark K, Bartlett DH, Kato C (2006) Fractionation of carbon isotopes in
878 biosynthesis of fatty acids by a piezophilic bacterium *Moritella japonica* strain DSK1.
879 *Geochimica Et Cosmochimica Acta* 70:1753-1760
- 880 Fry B, Jannasch HW, Molyneaux SJ, Wirsen CO, Muramoto JA, King S (1991) Stable Isotope
881 Studies of the Carbon Nitrogen and Sulfur Cycles in the Black Sea and the Cariaco Trench.
882 *Deep-Sea Research Part A Oceanographic Research Papers* 38:S1003-S1020
- 883 Gebruk A, Krylova E, Lein A, Vinogradov G, Anderson E, Pimenov N, Cherkashev G, Crane K
884 (2003) Methane seep community of the Håkon Mosby mud volcano (the Norwegian Sea):
885 composition and trophic aspects. *Sarsia: North Atlantic Marine Science* 88:394-403
- 886 Georgieva M, Wiklund H, Bell JB, Eilersten MH, Mills RA, Little CTS, Glover AG (2015) A
887 chemosynthetic weed: the tubeworm *Sclerolinum contortum* is a bipolar, cosmopolitan
888 species. *BMC Evolutionary Biology* 15:280



- 889 Gollner S, Govenar B, Fisher CR, Bright M (2015) Size matters at deep-sea hydrothermal vents:
890 different diversity and habitat fidelity patterns of meio- and macrofauna. *Marine Ecology*
891 *Progress Series* 520:57-66
- 892 Guezennec J, Fiala-Medioni A (1996) Bacterial abundance and diversity in the Barbados Trench
893 determined by phospholipid analysis. *Microbiology Ecology* 19:83-93
- 894 Guezennec J, Ortega-Morales O, Raguenes G, Geesey G (1998) Bacterial colonization of artificial
895 substrate in the vicinity of deep-sea hydrothermal vents. *FEMS Microbiology Ecology*
896 26:89-99
- 897 Hayes JM (2001) Fractionation of carbon and hydrogen isotopes in biosynthetic processes.
898 *Reviews in Mineralogy & Geochemistry* 43:225-277
- 899 Henley SF, Annett AL, Ganeshram RS, Carson DS, Weston K, Crosta X, Tait A, Dougans J, Fallick
900 AE, Clarke A (2012) Factors influencing the stable carbon isotopic composition of
901 suspended and sinking organic matter in the coastal Antarctic sea ice environment.
902 *Biogeosciences* 9:1137-1157
- 903 Hothorn T, van de Wiel MA, Zeilis A (2015) Package 'Coin': Conditional Inference Procedures in
904 a Permutation Test Framework. *cranr-projectorg*
- 905 Hugler M, Sievert SM (2011) Beyond the Calvin cycle: autotrophic carbon fixation in the ocean.
906 *Annual review of marine science* 3:261-289
- 907 Iken K, Brey T, Wand U, Voight J, Junghans P (2001) Trophic relationships in the benthic
908 community at Porcupine Abyssal Plain (NE Atlantic): a stable isotope analysis. *Progress*
909 *in Oceanography* 50:383-405
- 910 Jackson AL, Inger R, Parnell AC, Bearhop S (2011) Comparing isotopic niche widths among and
911 within communities: SIBER - Stable Isotope Bayesian Ellipses in R. *The Journal of animal*
912 *ecology* 80:595-602
- 913 Jaeschke A, Eickmann B, Lang SQ, Bernasconi SM, Strauss H, Fruh-Green GL (2014) Biosignatures
914 in chimney structures and sediment from the Loki's Castle low-temperature
915 hydrothermal vent field at the Arctic Mid-Ocean Ridge. *Extremophiles* 18:545-560
- 916 Jeffreys RM, Fisher EH, Gooday AJ, Larkin KE, Billett DSM, Wolff GA (2015) The trophic and
917 metabolic pathways of foraminifera in the Arabian Sea: evidence from cellular stable
918 isotopes. *Biogeosciences* 12:1781-1797
- 919 Kallmeyer J, Boetius A (2004) Effects of Temperature and Pressure on Sulfate Reduction and
920 Anaerobic Oxidation of Methane in Hydrothermal Sediments of Guaymas Basin. *Applied*
921 *and environmental microbiology* 70:1231-1233
- 922 Kharlamenko VI, Zhukova NV, Khotimchenko SV, Svetashev VI, Kamenev GM (1995) Fatty-acids
923 as markers of food sources in a shallow-water hydrothermal ecosystem (Kraternaya
924 Bight, Yankich island, Kurile Islands). *Marine Ecology Progress Series* 120:231-241
- 925 Kiel S (2016) A biogeographic network reveals evolutionary links between deep-sea
926 hydrothermal vent and methane seep faunas. *Proceedings of the Royal Society B:*
927 *Biological Sciences* 283
- 928 Klinkhammer GP, Chin CS, Keller RA, Dahlmann A, Sahling H, Sarthou G, Petersen S, Smith F
929 (2001) Discovery of new hydrothermal vent sites in Bransfield Strait, Antarctica. *Earth*
930 *and Planetary Science Letters* 193:395-407
- 931 Klouche N, Basso O, Lascourrèges J-F, Cavol J-L, Thomas P, Fauque G, Fardeau M-L, Magot M
932 (2009) *Desulfocurvus vexinensis* gen. nov., sp. nov., a sulfate-reducing bacterium isolated
933 from a deep subsurface aquifer. *International Journal of Systematic and Evolutionary*
934 *Microbiology* 30:3100-3104
- 935 Kohring L, Ringelberg D, Devereux R, Stahl DA, Mittelman MW, White DC (1994) Comparison of
936 phylogenetic relationships based on phospholipid fatty acid profiles and ribosomal RNA



- 937 sequence similarities among dissimilatory sulfate-reducing bacteria. *Fems Microbiology*
938 *Letters* 119:303-308
- 939 Koranda M, Kaiser C, Fuchslueger L, Kitzler B, Sessitsch A, Zechmeister-Boltenstern S, Rickhter
940 A (2013) Fungal and bacterial utilization of organic substrates depends on substrate
941 complexity and N availability. In: Dieckmann U (ed). *International Institute for Applied*
942 *Systems Analysis*, Laxenburg, Austria
- 943 Larsen K (2006) Tanaidacea (Crustacea; Peracarida) from chemically reduced habitats—the
944 hydrothermal vent system of the Juan de Fuca Ridge, Escabana Trough and Gorda Ridge,
945 northeast Pacific. *Zootaxa* 1164:1-33
- 946 Layman CA, Arrington DA, Montaña CG, Post DM (2007) Can Stable Isotope Ratios Provide For
947 Community-Wide Measures of Trophic Structure? *Ecology* 88:42-48
- 948 Levin LA, Baco AR, Bowden D, Colaço A, Cordes E, Cunha MR, Demopoulos A, Gobin J, Grupe B,
949 Le J, Metaxas A, Netburn A, Rouse GW, Thurber AR, Tunnicliffe V, Van Dover C, Vanreusel
950 A, Watling L (2016) Hydrothermal Vents and Methane Seeps: Rethinking the Sphere of
951 Influence. *Frontiers in Marine Science* 3:72
- 952 Levin LA, Mendoza GF, Konotchick T, Lee R (2009) Macrobenthos community structure and
953 trophic relationships within active and inactive Pacific hydrothermal sediments. *Deep*
954 *Sea Research Part II: Topical Studies in Oceanography* 56:1632-1648
- 955 Levin LA, Ziebis W, Mendoza GF, Bertics VJ, Washington T, Gonzalez J, Thurber AR, Ebbed B, Lee
956 RW (2013) Ecological release and niche partitioning under stress: Lessons from
957 dorvilleid polychaetes in sulfidic sediments at methane seeps. *Deep-Sea Research Part II-*
958 *Topical Studies in Oceanography* 92:214-233
- 959 Liao L, Wankel SD, Wu M, Cavanaugh CM, Girguis PR (2014) Characterizing the plasticity of
960 nitrogen metabolism by the host and symbionts of the hydrothermal vent
961 chemoautotrophic symbioses *Ridgeia piscesae*. *Mol Ecol* 23:1544-1557
- 962 Macko SA, Estep MLF (1984) Microbial alteration of stable nitrogen and carbon isotopic
963 compositions of organic matter. *Organic Geochemistry* 6:787-790
- 964 Main CE, Ruhl HA, Jones DOB, Yool A, Thornton B, Mayor DJ (2015) Hydrocarbon contamination
965 affects deep-sea benthic oxygen uptake and microbial community composition. *Deep Sea*
966 *Research Part I: Oceanographic Research Papers* 100:79-87
- 967 Martens CS (1990) Generation of short chain organic acid anions in hydrothermally altered
968 sediments of the Guaymas Basin, Gulf of California. *Applied Geochemistry* 5:71-76
- 969 McCaffrey MA, Farrington JW, Repeta DJ (1989) Geo-chemical implications of the lipid
970 composition of *Thioploca* spp. from the Peru upwelling region - 15°S. *Organic*
971 *Geochemistry* 14
- 972 McClain CR, Schlacher TA (2015) On some hypotheses of diversity of animal life at great depths
973 on the sea floor. *Marine Ecology*:12288
- 974 Mehta MP, Baross JA (2006) Nitrogen Fixation at 92°C by a Hydrothermal Vent Archaeon. *Science*
975 314:1783-1786
- 976 Mincks SL, Smith CR, Jeffreys RM, Sumida PYG (2008) Trophic structure on the West Antarctic
977 Peninsula shelf: Detritivory and benthic inertia revealed by $\delta^{13}\text{C}$ and $\delta^{15}\text{N}$ analysis. *Deep*
978 *Sea Research Part II: Topical Studies in Oceanography* 55:2502-2514
- 979 Naraoka H, Naito T, Yamanaka T, Tsunogai U, Fujikura K (2008) A multi-isotope study of deep-
980 sea mussels at three different hydrothermal vent sites in the northwestern Pacific.
981 *Chemical Geology* 255:25-32
- 982 Ondov BD, Bergman NH, Phillippy AM (2011) Interactive metagenomic visualization in a Web
983 browser. *BMC Bioinformatics* 30:385
- 984 Parnell AC, Inger R, Bearhop S, Jackson AL (2010) Source partitioning using stable isotopes:
985 coping with too much variation. *PLoS One* 5:e9672



- 986 Parrish CC (2013) Lipids in Marine Ecosystems. *ISRN Oceanography* 2013:16
- 987 Petersen S, Herzig PM, Schwarz-Schampera U, Hannington MD, Jonasson IR (2004)
- 988 Hydrothermal precipitates associated with bimodal volcanism in the Central Bransfield
- 989 Strait, Antarctica. *Mineralium Deposita* 39:358-379
- 990 Phillips DL, Inger R, Bearhop S, Jackson AL, Moore JW, Parnell AC, Semmens BX, Ward EJ (2014)
- 991 Best practices for use of stable isotope mixing models in food-web studies. *Canadian*
- 992 *Journal of Zoology* 92:823-835
- 993 Pina-Ochoa E, Koho KA, Geslin E, Risgaard-Petersen N (2010) Survival and life strategy of the
- 994 foraminiferan *Globobulimina turgida* though nitrate storage and denitrification. *Marine*
- 995 *Ecology Progress Series* 417:39-49
- 996 Pond DW, Bell MV, Dixon DR, Fallick AE, Segonzac M, Sargent JR (1998) Stable-Carbon-Isotope
- 997 Composition of Fatty Acids in Hydrothermal Vent Mussels Containing Methanotrophic
- 998 and Thiotrophic Bacterial Endosymbionts. *Applied and environmental microbiology*
- 999 64:370-375
- 1000 Portail M, Olu K, Dubois SF, Escobar-Briones E, Gelinas Y, Menot L, Sarrazin J (2016) Food-Web
- 1001 Complexity in Guaymas Basin Hydrothermal Vents and Cold Seeps. *PLoS One*
- 1002 11:e0162263
- 1003 R Core Team (2013) R: A Language and environment for statistical computing. R Foundation for
- 1004 Statistical Computing, Vienna, Austria <http://www.R-project.org/>.
- 1005 Rau GH (1981) Low $^{15}\text{N}/^{14}\text{N}$ in hydrothermal vent animals: ecological implications. *Nature*
- 1006 289:484-485
- 1007 Reid WDK, Sweeting CJ, Wigham BD, McGill RAR, Polunin NVC (2016) Isotopic niche variability
- 1008 in macroconsumers of the East Scotia Ridge (Southern Ocean) hydrothermal vents: what
- 1009 more can we learn from an ellipse? *Marine Ecology Progress Series*:13-24
- 1010 Reid WDK, Sweeting CJ, Wigham BD, Zwirgmaier K, Hawkes JA, McGill RAR, Linse K, Polunin
- 1011 NVC (2013) Spatial Differences in East Scotia Ridge Hydrothermal Vent Food Webs:
- 1012 Influences of Chemistry, Microbiology and Predation on Trophodynamics. *Plos One* 8
- 1013 Reid WDK, Wigham BD, McGill RAR, Polunin NVC (2012) Elucidating trophic pathways in benthic
- 1014 deep-sea assemblages of the Mid-Atlantic Ridge north and south of the Charlie-Gibbs
- 1015 Fracture Zone. *Marine Ecology Progress Series* 463:89-103
- 1016 Rennie MD, Ozersky T, Evans DO (2012) Effects of formalin preservation on invertebrate stable
- 1017 isotope values over decadal time scales. *Canadian Journal of Zoology* 90:1320-1327
- 1018 Rodrigues CF, Hilário A, Cunha MR (2013) Chemosymbiotic species from the Gulf of Cadiz (NE
- 1019 Atlantic): distribution, life styles and nutritional patterns. *Biogeosciences* 10:2569-2581
- 1020 Sahling H, Wallman K, Dähmann A, Schmaljohann R, Petersen S (2005) The physicochemical
- 1021 habitat of *Sclerolinum sp.* at Hook Ridge hydrothermal vent, Bransfield Strait, Antarctica.
- 1022 *Limnology & Oceanography* 50:598-606
- 1023 Schlesner H (2015) Blastopirellula. *Bergey's Manual of Systematics of Archaea and Bacteria*.
- 1024 John Wiley & Sons, Ltd
- 1025 Schmaljohann R, Faber E, Whittar MJ, Dando PR (1990) Co-existence of methane- and sulphur-
- 1026 based endosymbioses between bacteria and invertebrates at a site in the Skagerrak.
- 1027 *Marine Ecology Progress Series* 61:11-124
- 1028 Schmaljohann R, Flügel HJ (1987) Methane-oxidizing bacteria in Pogonophora. *Sarsia* 72:91-98
- 1029 Sellanes J, Zapata-Hernández G, Pantoja S, Jessen GL (2011) Chemosynthetic trophic support for
- 1030 the benthic community at an intertidal cold seep site at Mocha Island off central Chile.
- 1031 *Estuarine, Coastal and Shelf Science* 95:431-439
- 1032 Soto LA (2009) Stable carbon and nitrogen isotopic signatures of fauna associated with the deep-
- 1033 sea hydrothermal vent system of Guaymas Basin, Gulf of California. *Deep Sea Research*
- 1034 Part II: Topical Studies in Oceanography 56:1675-1682



- 1035 Southward A, J., Southward EC, Brattegard T, Bakke T (1979) Further Experiments on the value
1036 of Dissolved Organic Matter as Food for *Siboglinum fjordicum* (Pogonophora). Journal of
1037 Marine Biological Association of the United Kingdom 59:133-148
- 1038 Sweetman AK, Levin LA, Rapp HT, Schander C (2013) Faunal trophic structure at hydrothermal
1039 vents on the southern Mohn's Ridge, Arctic Ocean. Marine Ecology Progress Series
1040 473:115
- 1041 Tarasov VG, Gebruk AV, Mironov AN, Moskalev LI (2005) Deep-sea and shallow-water
1042 hydrothermal vent communities: Two different phenomena? Chemical Geology 224:5-39
- 1043 Teske A, Callaghan AV, LaRowe DE (2014) Biosphere frontiers of subsurface life in the
1044 sedimented hydrothermal system of Guaymas Basin. Frontiers in microbiology 5:362
- 1045 Teske A, Hinrichs KU, Edgcomb V, de Vera Gomez A, Kysela D, Sylva SP, Sogin ML, Jannasch HW
1046 (2002) Microbial Diversity of Hydrothermal Sediments in the Guaymas Basin: Evidence
1047 for Anaerobic Methanotrophic Communities. Applied and environmental microbiology
1048 68:1994-2007
- 1049 Thornhill DJ, Wiley AA, Campbell AL, Bartol FF, Teske A, Halanych KM (2008) Endosymbionts of
1050 *Siboglinum fjordicum* and the Phylogeny of Bacterial Endosymbionts in Siboglinidae
1051 (Annelida). Biological Bulletin 214:135-144
- 1052 Thornton B, Zhang Z, Mayes RW, Högberg MN, Midwood AJ (2011) Can gas chromatography
1053 combustion isotope ratio mass spectrometry be used to quantify organic compound
1054 abundance? Rapid Communications in Mass Spectrometry 25:2433-2438
- 1055 Tyler PA, Connelly DP, Copley JT, Linse K, Mills RA, Pearce DA, Aquilina A, Cole C, Glover AG,
1056 Green DR, Hawkes JA, Hepburn L, Herrera S, Marsh L, Reid WD, Roterman CN, Sweeting
1057 CJ, Tate A, Woulds C, Zwirgmaier K (2011) RRS *James Cook* cruise JC55: Chemosynthetic
1058 Ecosystems of the Southern Ocean. BODC Cruise Report
- 1059 Valls M, Olivar MP, Fernández de Puelles ML, Molí B, Bernal A, Sweeting CJ (2014) Trophic
1060 structure of mesopelagic fishes in the western Mediterranean based on stable isotopes of
1061 carbon and nitrogen. Journal of Marine Systems 138:160-170
- 1062 Vetter RD, Fry B (1998) Sulfur contents and sulfur-isotope compositions of thiotrophic
1063 symbioses in bivalve molluscs and vestimentiferan worms. Marine Biology 132:453-460
- 1064 Veuger B, van Oevelen D, Middelburg JJ (2012) Fate of microbial nitrogen, carbon, hydrolysable
1065 amino acids, monosaccharides, and fatty acids in sediment. Geochimica Et Cosmochimica
1066 Acta 83
- 1067 Walker BD, McCarthy MD, Fisher AT, Guilderson TP (2008) Dissolved inorganic carbon isotopic
1068 composition of low-temperature axial and ridge-flank hydrothermal fluids of the Juan de
1069 Fuca Ridge. Marine Chemistry 108:123-136
- 1070 Wang Q, Garrity GM, Tiedje JM, Cole JR (2007) Naïve Bayesian Classifier for Rapid Assignment
1071 of rRNA sequences into the New Bacterial Taxonomy. Applied Environmental
1072 Microbiology 73:5261-5267
- 1073 Whitaker D, Christmann M (2013) Package 'clustsig'. cranr-projectorg
- 1074 Whitticar MJ (1999) Carbon and Hydrogen isotope systematics of bacterial formation and
1075 oxidation of methane. Chemical Geology 161:291-314
- 1076 Whitticar MJ, Suess E (1990) Hydrothermal hydrocarbon gases in the sediments of the King
1077 George Basin, Bransfield Strait, Antarctica. Applied Geochemistry 5:135-147
- 1078 Woolley SNC, Tittensor DP, Dunstan PK, Guillera-Arroita G, Lahoz-Monfort JJ, Wintle BA, Worm
1079 B, O'Hara TD (2016) Deep-sea diversity patterns are shaped by energy availability.
1080 Nature
- 1081 Wu Y, Cao Y, Wang C, Wu M, Aharon O, Xu X (2014) Microbial community structure and
1082 nitrogenase gene diversity of sediment from a deep-sea hydrothermal vent field on the
1083 Southwest Indian Ridge. Acta Oceanologica Sinica 33:94-104

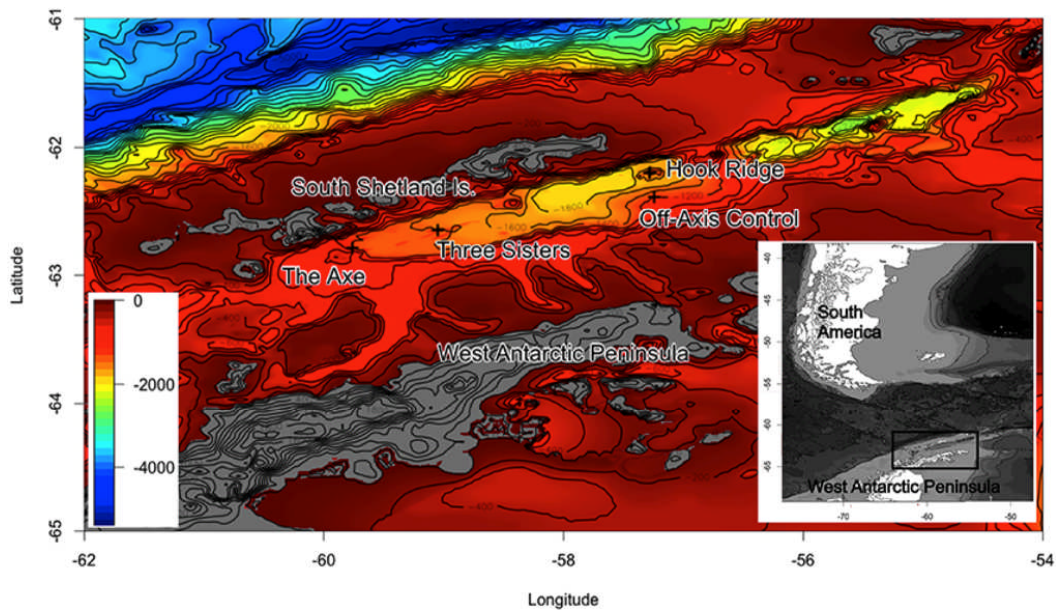


- 1084 Würzberg L, Peters J, Schüller M, Brandt A (2011) Diet insights of deep-sea polychaetes derived
1085 from fatty acids analyses. *Deep Sea Research Part II* 58:153-162
- 1086 Yamanaka T, Sakata S (2004) Abundance and distribution of fatty acids in hydrothermal vent
1087 sediments of the western Pacific Ocean. *Organic Geochemistry* 35:573-582
- 1088 Yamanaka T, Shimamura S, Nagashio H, Yamagami S, Onishi Y, Hyodo A, Mampuku M, Mizota C
1089 (2015) A Compilation of the Stable Isotopic Compositions of Carbon, Nitrogen, and Sulfur
1090 in Soft Body Parts of Animals Collected from Deep-Sea Hydrothermal Vent and Methane
1091 Seep Fields: Variations in Energy Source and Importance of Subsurface Microbial
1092 Processes in the Sediment-Hosted Systems. In: Ishibashi J, Okino K, Sunamura M (eds)
1093 *Subseafloor Biosphere Linked to Hydrothermal Systems*. SpringerOpen, Tokyo
- 1094 Yorisue T, Inoue K, Miyake H, Kojima S (2012) Trophic structure of hydrothermal vent
1095 communities at Myojin Knoll and Nikko Seamount in the northwestern Pacific:
1096 Implications for photosynthesis-derived food supply. *Plankton and Benthos Research*
1097 7:35-40
- 1098 Young JN, Bruggeman J, Rickaby REM, Erez J, Conte M (2013) Evidence for changes in carbon
1099 isotopic fractionation by phytoplankton between 1960 and 2010. *Global Biogeochemical*
1100 *Cycles* 27:505-515
- 1101
- 1102



1103 10. Figure captions

1104

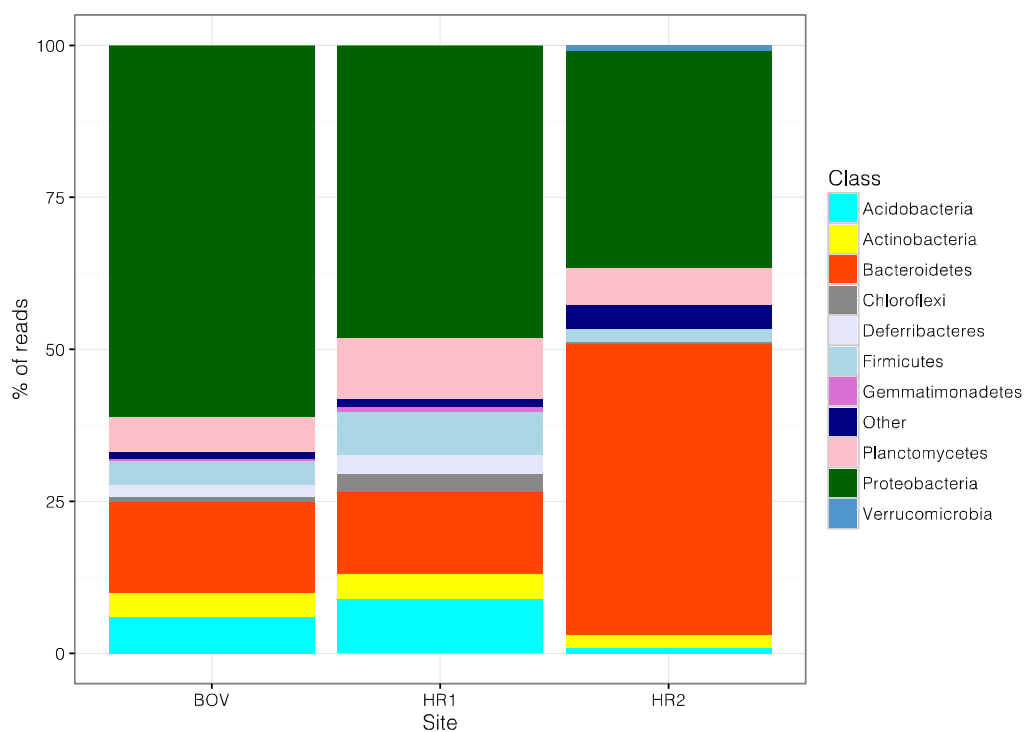


1105

1106 Figure 1 – Sampling sites (after Bell et al. 2016b)

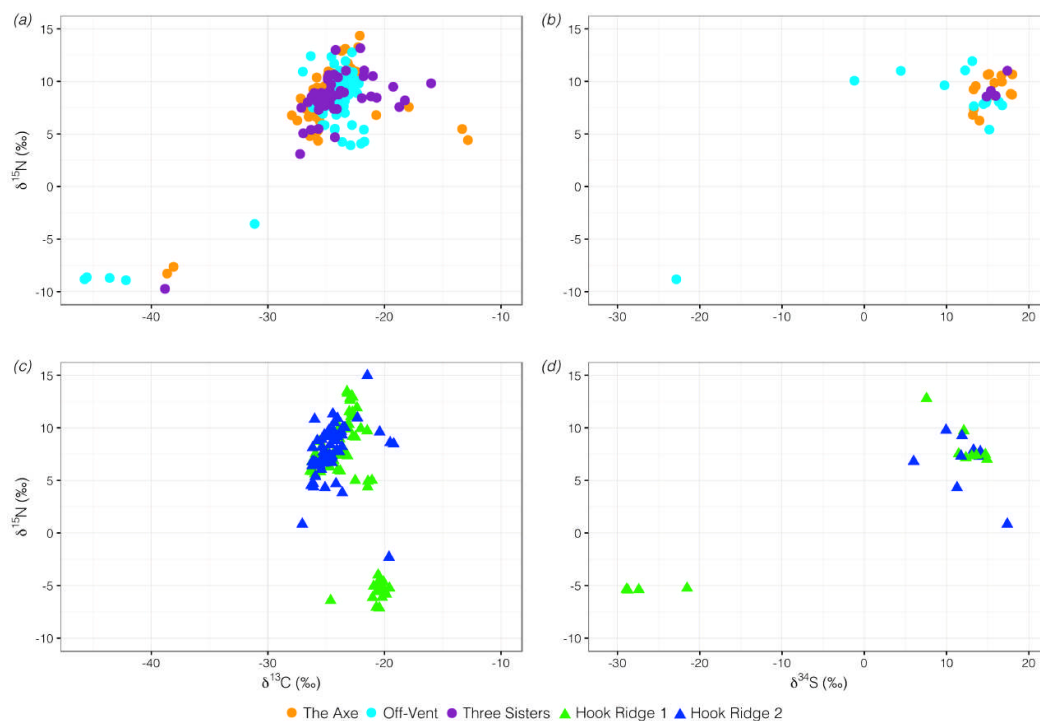


1107



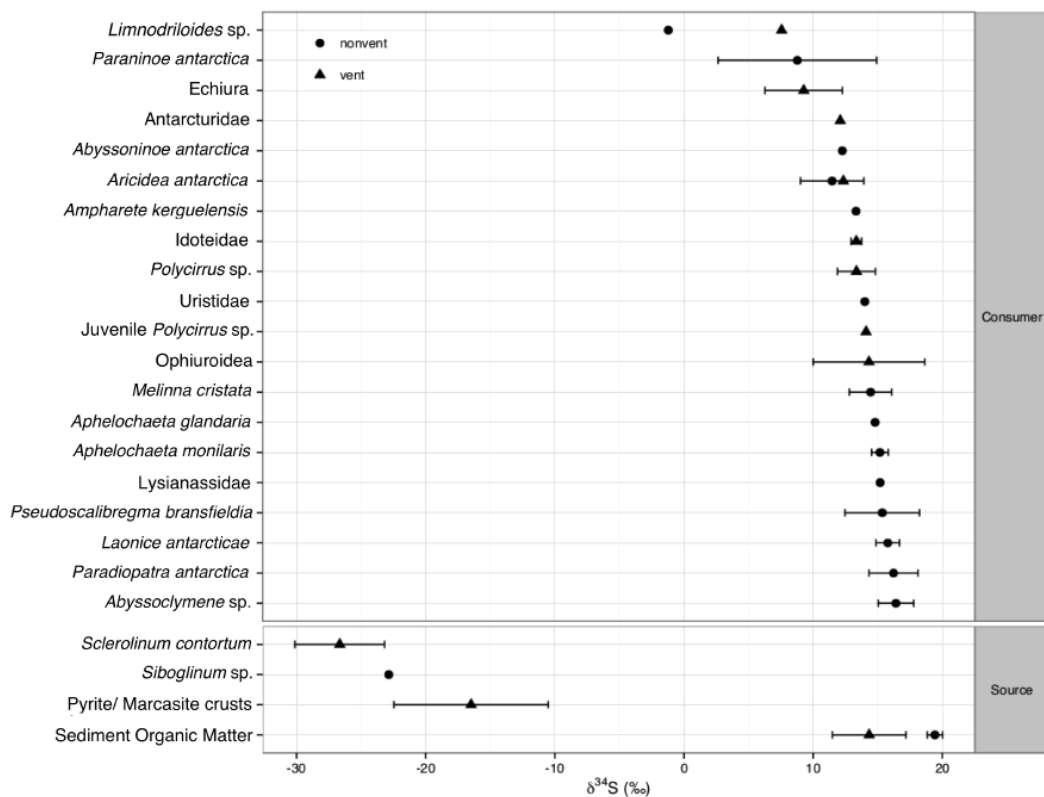
1108

1109 Figure 2 – Microbial composition (classes) at the off-vent/ off-axis site (BOV) and the two Hook
1110 Ridge sites (HR1 and HR2). Archaea excluded from figure as they only accounted for 0.008 % of
1111 reads at HR2 and were not found elsewhere.



1112

1113 Figure 3 – Carbon-Nitrogen and Sulphur-Nitrogen biplots for bulk isotopic signatures of benthos,
 1114 separated into non-vent (top) and vent sites (bottom). Excepting one value from the off-vent site
 1115 (for a peracarid species), all values with $\delta^{15}\text{N}$ of < 0 were siboglinid species (*Sclerolinum*
 1116 *contortum* from the vent sites and *Siboglinum* spp. from the non-vent sites).

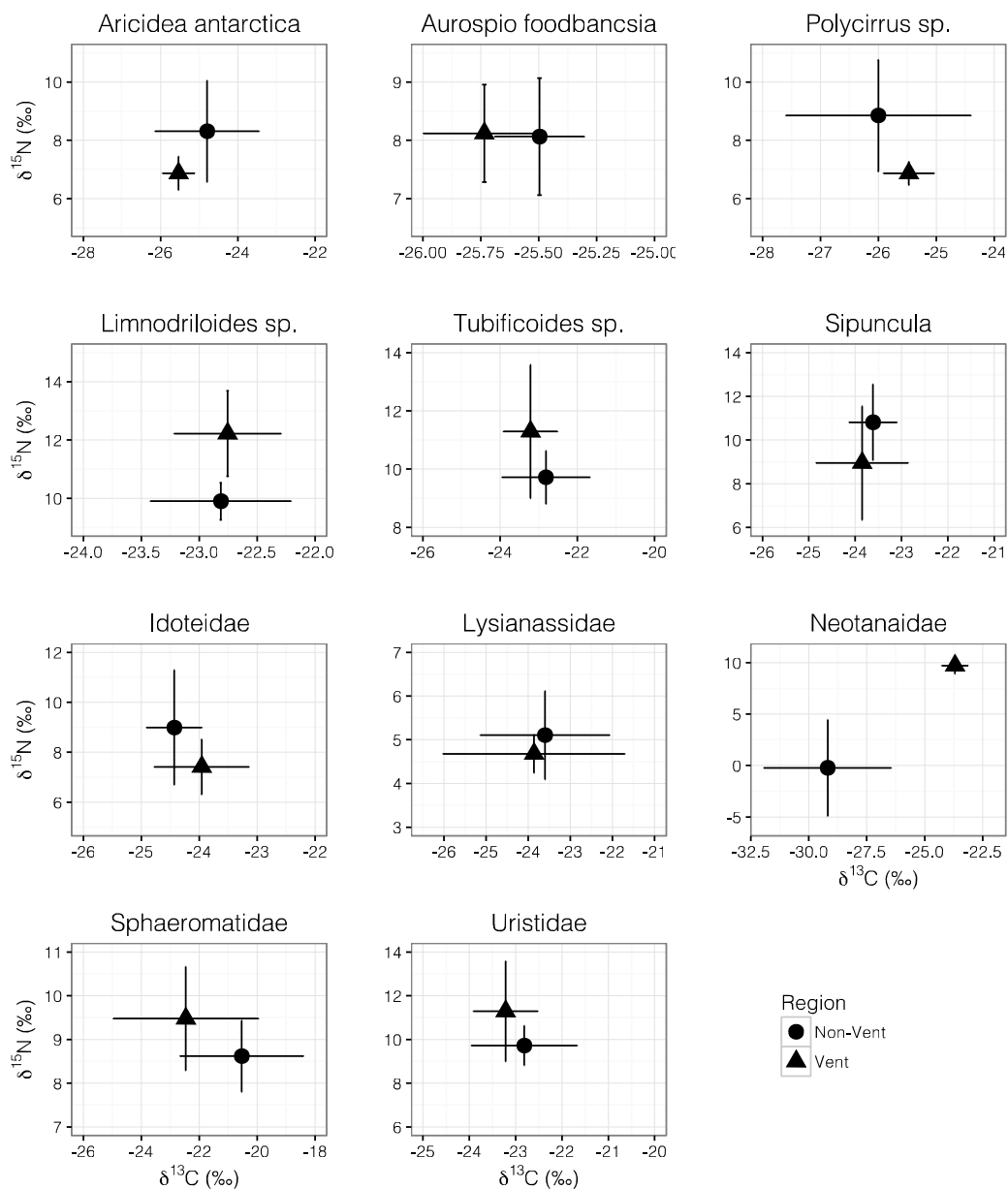


1117

1118 Figure 4 – Plot of $\delta^{34}\text{S}$ measurements by discriminated by species and habitat (vent/ non-vent \pm

1119 1 s.d.). Data for $\delta^{34}\text{S}$ in crusts from Petersen et al. (2004)

1120



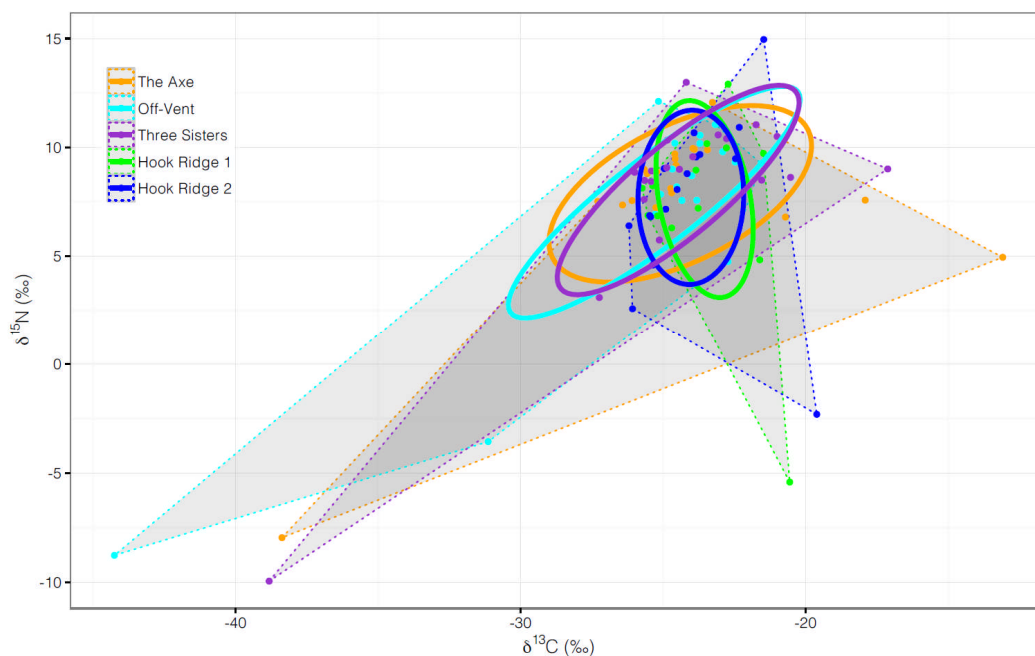
1121

1122 Figure 5– Biplot of CN isotopic data from species sampled both at vents and non-vent

1123 background regions. Mean \pm standard deviation, X-Y scales vary

1124

1125



1126

1127 Figure 6 – Faunal isotopic signatures (mean per species), grouped by site with total area (shaded

1128 area marked by dotted lines) and sample-size corrected standard elliptical area (solid lines)

1129

1130



1131 11. Tables

Site	Depth (m)	Hydrothermally active?	References
The Axe (AXE)	1024	No	(Dählmann et al. 2001,
Off-Vent (BOV)	1150	No	Klinkhammer et al. 2001, Sahling
Three Sisters (TS)	1311	No	et al. 2005, Aquilina et al. 2013,
Hook Ridge 1 (HR1)	1174	Low activity (9 cm yr ⁻¹)	Aquilina et al. 2014, Bell et al.
Hook Ridge 2 (HR2)	1054	High Activity (34 cm yr ⁻¹)	2016b)

1132

1133 Table 1 – Site descriptions and associated references



1134

Isotope	Species	Idoteidae	<i>Polycirrus</i> sp.	<i>Aphelochaeta</i> <i>glandaria</i>	Phyllodocida sp.
	Treatment	0.1M HCl	0.1M HCl	0.1M HCl	1.0M HCl
$\delta^{13}\text{C}$ (‰)	Difference in mean	1.6	0.2	0.4	0.9
	σ untreated	0.7	0.3	0.2	0.5
	σ treated	0.7	0.3	0.2	0.2
	Population range	2.9	3.0	2.7	-
$\delta^{15}\text{N}$ (‰)	Difference in mean	0.9	0.2	0.1	0.9
	σ untreated	0.2	0.3	0.2	0.4
	σ treated	1.0	0.2	0.2	0.3
	Population range	3.4	4.6	5.8	-
$\delta^{34}\text{S}$ (‰)	Difference in mean	-	-	0.4	1.1
	σ untreated	-	-	0.4	0.8
	σ treated	-	-	0.7	1.4
	Population range	-	-	2.3	-

1135

1136 Table 2 – Differences in isotopic values and standard deviation (σ) of ethanol preserved fauna
 1137 sampled during JC55 in response to acid treatment, compared with population ranges of
 1138 untreated samples. Phyllodocida sp. was a single large specimen, used only as part of
 1139 preliminary experiments. Data rounded to 1 d.p. to account for measurement error.

1140



1141

PLFA	Bransfield Off-Vent			Three Sisters		
	nM g ⁻¹	%	δ ¹³ C (‰)	nM g ⁻¹	%	δ ¹³ C (‰)
i14:0	0.03	0.12	-22.0	0.02	0.09	-28.0
14:0	0.80	3.04	-31.2	0.83	3.43	-30.9
i15:0	0.76	2.89	-28.6	0.76	3.13	-28.1
a15:0	1.06	4.03	-28.4	1.06	4.39	-27.7
15:0	0.30	1.13	-29.3	0.19	0.77	-29.8
i16:1	0.11	0.44	-31.4	0.02	0.10	-20.3
16:1w11c	0.00	0.00	n.d.	0.06	0.24	-23.1
i16:0	0.34	1.30	-28.5	0.30	1.24	-27.8
16:1w11t	0.78	2.98	-24.4	0.66	2.75	-25.0
16:1w7c	3.98	15.19	-28.9	3.37	13.95	-28.1
16:1w5c	1.12	4.27	-34.1	0.96	3.99	-34.0
16:0	4.29	16.37	-31.1	3.80	15.73	-30.0
br17:0	0.00	0.00	n.d.	0.00	0.00	n.d.
10-Me-16:0	0.46	1.77	-28.5	0.45	1.87	-29.1
i17:0	0.08	0.32	-33.2	0.20	0.84	-29.8
a17:0	0.25	0.97	-31.9	0.21	0.87	-31.3
12-Me-16:0	0.25	0.94	-32.9	0.21	0.86	-31.6
17:1w8c	0.13	0.50	-34.1	0.11	0.44	-31.3
17:0cy	0.33	1.26	-36.2	0.27	1.10	-32.8
17:0	0.15	0.56	-40.0	0.08	0.33	-50.4
10-Me-17:0	0.00	0.00	n.d.	0.00	0.00	n.d.
18:3w6,8,13	0.67	2.55	-34.6	0.69	2.87	-33.8
18:2w6,9	0.12	0.46	-27.8	0.09	0.36	-52.2
18:1w9	1.13	4.30	-30.0	1.33	5.50	-29.9
18:1w7	4.42	16.85	-29.0	3.84	15.91	-29.1
18:1w(10 or 11)	2.33	8.88	-30.1	2.26	9.36	-29.9
18:0	0.66	2.50	-30.6	0.54	2.22	-30.6
19:1w6	0.03	0.12	-23.5	0.03	0.12	-30.1
10-Me-18:0	0.00	0.00	n.d.	0.00	0.00	n.d.
19:1w8	0.11	0.42	-56.6	0.17	0.69	-37.5
19:0cy	0.20	0.77	-35.6	0.20	0.83	-34.8
20:4(n-6)	0.14	0.55	-40.0	0.20	0.83	-34.1
20:5(n-3)	0.41	1.57	-38.0	0.30	1.23	-39.3
20:1(n-9)	0.42	1.60	-31.5	0.41	1.71	-33.7
22:6(n-3)	0.22	0.83	-34.1	0.43	1.77	-30.0
22:1(n-9)	0.10	0.39	-31.3	0.10	0.41	-29.9
24:1(n-9)	0.03	0.12	-28.7	0.02	0.07	-29.7
Total	26.23			24.15		
Average	0.71		-30.5	0.65		-30.1



	mg C m ⁻²	$\delta^{13}\text{C}$ (‰)	mg C m ⁻²	$\delta^{13}\text{C}$ (‰)
Bacterial Biomass	134.50	-26.8	197.12	-26.4

1142

1143

PLFA	Hook Ridge 1		Hook Ridge 2		Range	
	nM g ⁻¹	$\delta^{13}\text{C}$ (‰)	nM g ⁻¹	%	$\delta^{13}\text{C}$ (‰)	$\delta^{13}\text{C}$ (‰)
i14:0	0.03	-15.7	0.10	0.80	-28.8	-13.1
14:0	0.80	-32.7	0.80	6.40	-29.6	-3.1
i15:0	0.76	-29.7	0.40	3.20	-28.1	-1.7
a15:0	1.06	-29.1	0.90	7.20	-28.9	-1.4
15:0	0.30	-29.0	0.30	2.40	-28.3	-1.5
i16:1	0.11	-27.6	0.00	0.00	n.d.	-11.1
16:1 ω 11c	0.00	-17.4	0.00	0.00	n.d.	-5.7
i16:0	0.34	-29.4	0.20	1.60	-28.8	-1.6
16:1 ω 11t	0.78	-25.8	0.30	2.40	-8.7	-17.2
16:1 ω 7c	3.98	-29.2	2.50	20.00	-22.9	-6.3
16:1 ω 5c	1.12	-31.2	0.30	2.40	-24.3	-9.7
16:0	4.29	-31.8	3.30	26.40	-29.3	-2.5
br17:0	0.00	-22.9	0.00	0.00	-15.8	-7.2
10-Me-16:0	0.46	-30.3	0.20	1.60	-41.3	-12.8
i17:0	0.08	n.d.	0.00	0.00	n.d.	-3.4
a17:0	0.25	-29.0	0.20	1.60	-28.6	-3.4
12-Me-16:0	0.25	-28.6	0.10	0.80	-28.2	-4.7
17:1 ω 8c	0.13	-27.1	0.10	0.80	-27.2	-6.9
17:0cy	0.33	-32.3	0.20	1.60	-27.7	-8.5
17:0	0.15	-40.0	0.20	1.60	-30.8	-19.6
10-Me-17:0	0.00	-35.0	0.00	0.00	n.d.	0.00
18:3 ω 6,8,13	0.67	-31.2	0.50	4.00	-29.0	-5.6
18:2 ω 6,9	0.12	-30.0	0.30	2.40	-26.7	-25.5
18:1 ω 9	1.13	-29.6	0.40	3.20	-25.6	-4.4
18:1 ω 7	4.42	-29.9	0.60	4.80	-24.7	-5.1
18:1 ω (10 or 11)	2.33	-31.9	0.00	1.60	n.d.	-2.0
18:0	0.66	-29.4	0.30	0.00	-29.9	-1.2
19:1 ω 6	0.03	-26.2	0.00	2.40	n.d.	-6.6



10-Me-18:0	0.00	-25.4	0.00	0.00	n.d.	0.0
19:1 ω 8	0.11	-41.2	0.00	0.00	n.d.	-19.1
19:0cy	0.20	-30.5	0.10	0.00	-28.7	-6.9
20:4(n-6)	0.14	n.d.	0.00	0.80	n.d.	-5.9
20:5(n-3)	0.41	n.d.	0.00	0.00	n.d.	-1.3
20:1(n-9)	0.42	n.d.	0.00	0.00	n.d.	-2.2
22:6(n-3)	0.22	n.d.	0.00	0.00	n.d.	-4.2
22:1(n-9)	0.10	n.d.	0.00	0.00	n.d.	-1.4
24:1(n-9)	0.03	n.d.	0.00	0.00	n.d.	-1.0
Total	26.23		12.30			
Average	0.71	-30.3	0.33		-26.9	
	mg C m⁻²	$\delta^{13}\text{C}$ (‰)		mg C m⁻²	$\delta^{13}\text{C}$ (‰)	
Bacterial Biomass	534.55	-26.6		85.45	-23.1	

1144

1145 Table 3 – PLFA profiles from freeze-dried sediment (nM per g dry sediment). PLFA names relate
 1146 to standard notation (i = iso; a = anti-iso; first number = number of carbon atoms in chain; ω =
 1147 double bond; Me = methyl group). N.P. = Not present in sample. Total PLFA $\delta^{13}\text{C}$ measurements
 1148 weighted by concentration Bulk bacterial $\delta^{13}\text{C}$ estimated from average conversion factor of
 1149 3.7 ‰ (Boschker & Middelburg 2002). No data = n.d. Range measurements may be subject to
 1150 rounding error. N. B. Table split to conform to submission portal requirements.

1151



1152

Isotope	Vents ‰ (± S.D.)	Non-Vent ‰ (± S.D.)	Different? (T-Test, df = 3)
$\delta^{13}\text{C}$	-26.2 (± 0.4)	-25.8 (± 0.3)	No
$\delta^{15}\text{N}$	5.7 (± 0.7)	5.0 (± 0.3)	No
$\delta^{34}\text{S}$	14.3 (± 2.9)	19.4 (± 0.6)	Yes (T = 3.49, p < 0.05)

1153

1154 Table 4 – Mean isotopic signatures of sediment organic matter.



1155

Site	Ellipse				Θ	E	CD	Nearest Neighbour Distance	
	SEAc (‰ ²)	SEAB (‰ ²)	Cred. (95% ± ‰ ²)	TA (‰ ²)				Mean	S.D.
The Axe	49.3	45.0	19.9	161.6	0.67	0.85	3.59	1.76	4.17
Off-Vent	39.8	36.5	16.8	139.1	0.81	0.97	4.34	2.13	3.88
Three Sisters	35.5	32.6	14.7	110.2	0.86	0.95	3.85	1.93	3.78
Hook Ridge 1	23.1	20.7	11.2	42.6	-1.43	0.94	3.30	1.64	2.60
Hook Ridge 2	23.4	21.1	10.7	61.8	1.55	0.89	3.17	1.52	2.03
Mean									
Non-Vent	41.5	38.0	17.2	137.0	0.78	0.92	3.93	1.94	3.94
Vent	23.2	20.9	11.0	52.2	0.10	0.91	3.23	1.58	2.31

1156

Site	Centroid				
	$\delta^{13}\text{C}$ (‰)	$\delta^{15}\text{N}$ (‰)	$\delta^{34}\text{S}$ (‰)	dNr (‰)	dCr (‰)
The Axe	-24.4	7.9		20.0	25.3
Off-Vent	-25.3	7.5	8.1	20.9	22.7
Three Sisters	-24.5	8.0		22.9	21.7
Hook Ridge 1	-23.5	7.6	5.4	18.3	5.2
Hook Ridge 2	-24.0	7.7		17.3	6.6



Mean					
Non-Vent	-24.7	7.8		21.3	23.2
Vent	-23.8	7.7		17.8	5.9

1157

1158 Table 5 – Ellipse Area & Layman Metrics of benthos by site. SEAc = Sample-sized corrected
1159 standard elliptical area; SEA.B = Bayesian estimate of standard elliptical area; TA = Total hull
1160 area; E = Eccentricity; dNr = Nitrogen range; dCr = Carbon range; dSr = Sulphur range; CD =
1161 Centroid distance. Note: dSR reported only for Hook Ridge 1 and the off-vent site since $\delta^{34}\text{S}$
1162 values of siboglinids were only measured from these sites; hence dSr at other sites would be a
1163 considerable underestimate. As $\delta^{34}\text{S}$ values were comparatively under-representative, these
1164 values were not used in calculation of any other metric. Data rounded to 1 d.p. N. B. Table split
1165 to conform to submission portal requirements.